Co-funded by the
Erasmus+ Programme
of the European Union

Assessing the Influence of Urban Form on the Cooling Impacts of Urban Parks: A Case Study in Glasgow

Najma Yusuf Lelei

A thesis submitted for the Joint programme of
Master in Urban Climate & Sustainability

September 2023

Author	**Publication Type**	**Completion year**
Lelei, Najma Yusuf	Thesis	2023
	Number of pages: 87	
Supervisor I	**Supervisor II**	
Prof. Slobodan B Mickovski	Dr. Paul Carroll	

Title

Assessing the Influence of Urban Form on the Cooling Impacts of Urban Parks: A Case Study in Glasgow

Degree: Masters

Abstract

Urban Heat Island (UHI) effect has been a growing concern in the UK; therefore, the mitigation of such effects would contribute to sustainable urban development. A review of literature indicates that green infrastructure such as urban parks have proven to effectively regulate thermal comfort and aid in mitigating UHI effects. Parks cool their surroundings through heat exchange and shading. Several studies have explored the cooling effect of urban parks independently using various quantification methods without considering its surrounding spatial form. However, it is necessary to gain a comprehensive understanding of how the park cooling effect mechanism works on its surrounding built up area.

Using Remote Sensing, GIS, and Statistical analysis, 30 urban parks in Glasgow city were examined using buffer rings of 150 m and 300 m to investigate the influence of surrounding urban form to the park cooling effect (PCE). Park cooling effect (PCE) which is referred to as the cooling influence of parks on their surrounding built up areas, can be influenced by both park characteristics and their surrounding built up area. To understand the magnitude of cooling intensity of urban parks to their surrounding urban form, two parameters such as Park Cooling Intensity (PCI) and Park Cooling Distance (PCD) were used in this study. Landsat 8 TIR images were used to examine the Land Surface Temperature (LST) within the buffer zones to obtain PCI and PCD.

Park characteristics includes the area, perimeter, shape index and canopy cover were important factors used to determine the magnitude of cooling intensity of urban parks. Simultaneously, urban form parameters such as Mean Building Height (MBH), Floor Area Ratio (FAR), Canyon Aspect Ratio (H/W) and Sky View Factor (SVF) of the parks surrounding built up area were used to determine its influence on the potential cooling effect. The results found the average cooling intensity of the urban parks of sizes between 1.7 ha and 6.9 ha was 1.6°C while the cooling range was 252.7 m. Additionally, the relationship between the park characteristics and PCI including area, perimeter and NDVI showed a positive correlation except the shape index which negatively correlated with PCI. This suggest that with the increase in area, perimeter and vegetation in parks, there is an increase in PCE, while the decrease in shape complexity can enhance PCE. Urban form parameters however, showed negative correlation with PCI except the FAR which was positive correlated with PCI indicating that the increase in MBH, AR, SVF can decrease the cooling intensity of parks.

The results achieved in this study may contribute to the existing knowledge of park cooling effect and can provide guidance to policy makers on a more equitable urban park planning for climate adaptation on a local scale.

Keywords

UHI, Cooling effects, Urban parks, Urban morphology

Originality statement. I hereby declare that this master's dissertation is my own original work, does not contain other people's work without this being stated, cited and referenced, has not been submitted elsewhere in fulfilment of the requirements of this or any other award.	**Signature**

TABLE OF CONTENT

ACKNOWLEDGMENT

Firstly, I give all my gratitude to Allah, for bestowing endless blessings and wisdom upon me to get through this dissertation.

My deep gratitude goes to MUrCS consortium for giving me this exceptional opportunity to achieve one of my dreams. Thank you to all MUrCS partners; GCU, LAB Uni, HTWD and UHU for providing me with a stimulating and nurturing academic environment. Through MUrCS journey I have met wonderful people, visited great countries, and made unforgettable memories. All the academic staff of MUrCS have always been supportive throughout my academic journey. I am very grateful to be part of MUrCS team. MUrCS journey will be a story that I will always be excited to tell.

Secondly, I extend my appreciation to my colleagues and everyone who offered their assistance in this research, directly or indirectly. My sincere gratitude to my family for their understanding and tolerance throughout my academic journey.

Lastly, I want to thank myself for the dedication, perseverance and hard work that went into completing this master's thesis. I acknowledge the times when I felt overwhelmed or discouraged but managed to push through with resilience and self-motivation.

Thank you to everyone, including me.

LIST OF FIGURES

LIST OF TABLES

ABBREVIATIONS

ADMS – Atmospheric Dispersion Modelling System

AR – Aspect Ratio

BT – Brightness Temperature

CERC – Cambridge Environmental Research Consultants

DEM – Digital Elevation Model

DN – Digital Number

DSM – Digital Elevation Model

DTM – Digital Terrain Model

FAR – Floor Area Ratio

GCC – Glasgow City Council

GI – Green Infrastructure

GIS – Geographic Information System

LCZ – Local Climate Zone

LST – Land Surface Temperature

MBH – Mean Building Height

NDVI – Normalized difference vegetation index

NIR – Near Infrared

OS – Ordnance Survey

PCD – Park Cooling Distance

PCE – Park Cooling Effect

PCI – Park Cooling Intensity

SVF – Sky View Factor

TOA – Top of Atmospheric Spectral Radiance

UCL – Urban Canopy Layer

UHI – Urban Heat Island

UK – United Kingdom

UN – United Nations

USGS – United States Geological Survey

WUDAPT – World Urban Database Accept Portal Tools

CHAPTER 1. INTRODUCTION

1.1. Rationale

According to the UN, it is estimated that 68% of the world's population will live in cities by 2050 (UN, 2018). Due to this, cities have become a crucial concern with climate change. Urbanization and industrialization are causing dramatic changes in land use, land cover, and local climatic conditions around the world, which thereby exacerbates urban heat island (UHI) effects (Deilami, Kamruzzaman and Liu, 2017). The negative effects of UHI have resulted in increase in cooling energy consumption, physical discomfort and even death. If no action is taken, climate extremes are predicted to exceed current temperature levels across many parts of the world by 2100 (Power and D Delage, 2019). High temperatures and temperature extremes can have significant impacts on both the environment and urban residents.

In the UK, there has been a growing concern related to frequent heatwaves. In 2022, UK set a record high temperature at 40.3°C as the warmest year since 1884 according to Met Office (Homewood, 2023). Additionally, in the same year a record-breaking heatwave occurred in north Scotland of 35°C. Despite being historically cool, Scotland faces an increasing heat risk due to climate change (Undorf *et al.*, 2020). It is therefore imperative that adaptation measures be taken to cope with temperature extremes, especially in regions where heat waves are more frequent. Making cities inclusive, safe, resilient, and sustainable is crucial to create a more comfortable living environment for urban residents.

Green and blue infrastructures are considered effective and sustainable cooling strategies. They are also an integral part of the evaluation of urban life equity. In cities, urban parks play a crucial role in mitigating urban heat islands (Chen *et al.*, 2022). Several researchers have acknowledged their potential as natural cooling pathway in mitigating UHI intensity. However, increasing the number of large parks without limitation may not necessarily be an efficient way to alleviate urban heating in cities. Better planning and designing of urban parks in a more efficient way could improve both the environment and mitigate urban heat island effect. This is because a parks cooling range is greatly influenced by its landscape configuration, particularly the amount of impervious surface surrounding it. As the Park Cooling Effect (PCE) varies significantly according to the park characteristics and its surrounding built up area, it is vital to conduct a cooling equity assessment to provide more efficient cooling and environment justice (Tan and Samsudin, 2017a).

Numerous studies have quantified the cooling effect of parks independently using various cooling indicators, simulations, and calculation methods. However few studies have considered assessing PCE to its surrounding urban characteristics. Considering that urban areas have unique infrastructure layouts or form that alter microclimate in the Urban Canopy Layer (UCL), various urban forms can have an impact on PCE through radiation transfer and airflow dispersion (Lin *et al.*, 2015a). Therefore, it is necessary to assess the effect of urban form on PCE of urban parks to optimize its cooling effect. In the context of climate change, the importance of climate sensitive planning has been increasingly recognized. As a result, the current study seeks to provide key insights for urban park planning and design according to different urban forms to optimize parks cooling effect.

1.2. Aim and Objectives

This study aims to analyse how urban parks' cooling potential changes based on changing urban form, which may provide significant guidance for best urban parks' planning practices for mitigation and adaptation of urban heat island effects in Glasgow, UK.

To attain the stated goal, this study focuses on four objectives:

i. To develop a comprehensive understanding of the cooling impact of urban parks on the urban heat island intensity
ii. To quantify cooling effect of urban parks and identify the influencing factors.
iii. To analyse how the spatial form can influence the PCI
iv. To evaluate the link between urban morphology parameters, PCI and Urban Heat Island intensity.

1.3. Methodology Outline

The methodology approach of this study covers the following elements: Critical literature review, spatial and statistical analysis. This study uses Remote Sensing and GIS technique to analyse LST, vegetation cover and potential cooling effect using buffer analysis. It also intends to investigate the cooling impacts of urban parks in relation to its urban physical aspects. Software used in this research were: ArcGIS Pro 3.0, Microsoft Excel, Google Earth Pro, and SPSS

1.4. Dissertation Structure

This dissertation consists of six chapters:

Chapter 1 gives a brief overview of the research problem and its significance; it highlights the study's aim and objectives while underlining the scope of the study.

Chapter 2 presents a critical literature review related to UHI, urban morphology, and cooling effects of urban parks. It also gives an overview of Glasgow city.

Chapter 3 outlines the methodological approach to achieving the aim and objectives of this study.

Chapter 4 provides the results and analysis of the collected data.

Chapter 5 highlights a summary of findings and presents thorough discussion of the of the proposals. It also presents the potential implications for urban development and climate mitigation.

Chapter 6 concludes the study by summarizing the conclusions, limitations, and recommendation of the research.

CHAPTER 2. LITERATURE REVIEW

2.1. Overview of the UHI Phenomenon

Urban Heat Island (UHI) is a growing concern around the world due to the rising mean temperatures and heat waves. Urban areas with an absence of vegetation and natural landscape majorly contribute to the establishment of the urban heat island compared to rural areas. With the increase in urbanization along with impervious surfaces and anthropogenic heat production from buildings and vehicles, there is an increase in local temperatures and thus, UHI intensity. The urban heat island (UHI) effect can exacerbate warmth and temperature conditions in the summer to up to 8°C and it is more noticeable at night, exposing residents to heat stress (Akbari and Kolokotsa, 2016).

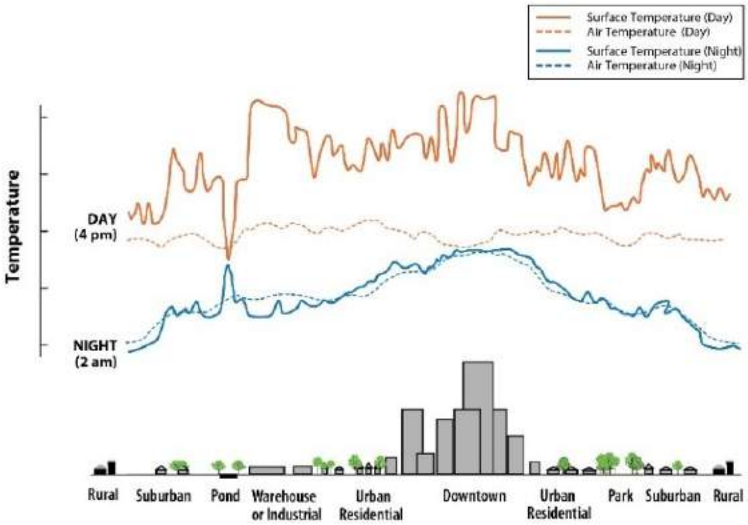

Figure 2.1 Urban Heat Island effects illustration (U.S. Environmental Protection Agency)

Such exposure poses threats to vulnerable groups particularly old people and children. When the vulnerable are exposed to extreme heat, they can suffer from heat-related illness such as heat stroke, heat rashes, heat cramps, heat exhaustion, and heat syncope. These illnesses may eventually even cause death. For instance, in 2022 the UK set a new record-high temperature of 40.3°C at Coningsby, Lincolnshire followed by the highest observed mortality, according to UK Health Security Agency (Excess mortality during heat-periods - Office for National Statistics). The same heatwave caused more than 15,000 deaths in Europe, according to the World Health Organization (WHO). Among those 4,500 deaths in Germany, 4,000 in Spain, 3,200 in the United Kingdom, and 1,000 in Portugal during the 3 months of summer (Excess mortality during heat periods - Office for National Statistics).

Over the last few decades, Scotland has experienced a warming trend and shifting rainfall with a projected temperature increase of 1.2 - 1.5°C by 2050 and more frequent heat waves. (Adaptation Scotland:: Climate trends and projections, 2021). Similarly, Glasgow has recorded the hottest summer since 1884 with urban areas being an average 4-6°C warmer due to the UHI effect (CLIMATE PROOFING GLASGOW Adaptation Strategies for Urban Overheating, 2021).

2.1.1. Causes of Urban Heat Island Effect

Factors causing the Urban Heat Island effect can be categorized into two; Uncontrollable and controllable factors as seen in Figure 2.2. Uncontrollable factors include those that are caused by atmospheric and natural environments. These are related to climatic conditions, weather, and geographic location of a place. However, controllable factors are the results of urbanization, urban morphology and design, and waste heat from human activities. Waste heat build-up from transportation and other mechanical activities contributes to the rising temperatures in cities causing UHI (Kamboj and Ali, 2021). The rise in temperature may result in heat stress and thermal discomfort in humans. Accordingly, there is an urgent need for cities to mitigate urban warming and its impacts.

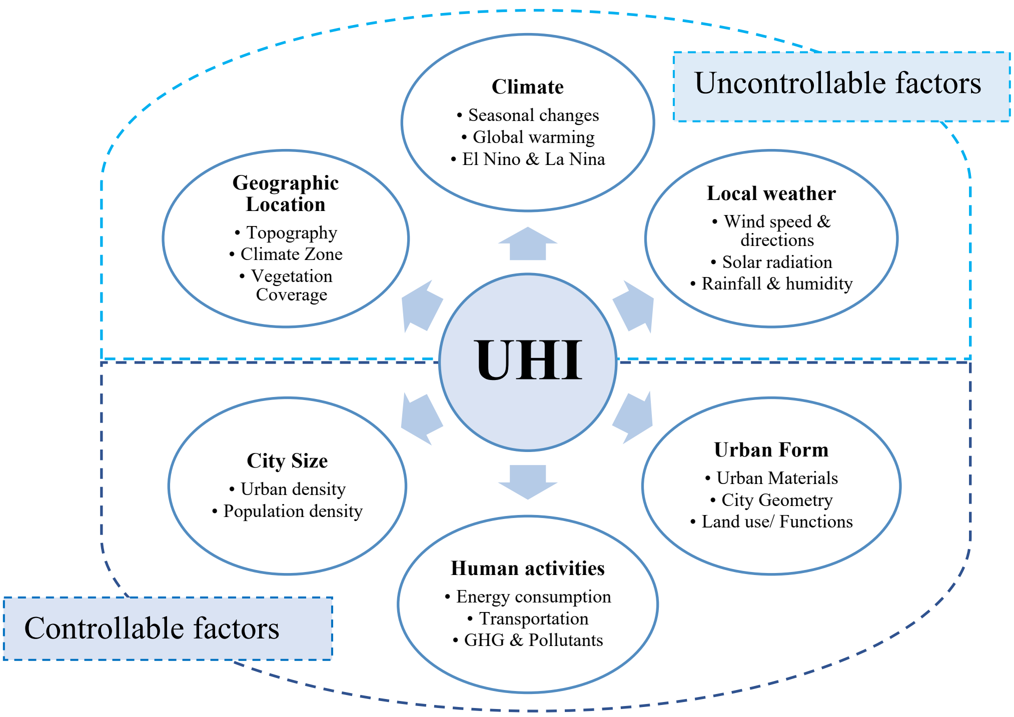

Figure 2.2 Factors contributing to the Urban Heat Island Effect.

2.1.2. Heat Mitigation Strategies

Scholars and policymakers have thus several active and passive strategies to mitigate the UHI effect. They can be broadly categorized into three different approaches. The first approach involves changing the thermal properties of urban materials that can be found in cities. For instance, changing the color of roofs and pavements to a lighter and more reflective color. This will reduce the amount of heat that is stored in the urban fabric because the energy is reflected back into the atmosphere.

The second approach includes changing the urban form. This approach encourages urban morphology design that minimizes heat gain, allowing maximum airflow and shading. Research has shown that the UHI intensity is greatly influenced by urban form (Liu *et al.*, 2022). Poor urban morphology may keep buildings from releasing the heat stored, resulting in temperature increase in the environment.

The third approach involves green infrastructure. Green infrastructure is highly considered an essential strategy for UHI mitigation. Researchers have also shown that the combination of multiple green infrastructure strategies provides great results in improving microclimate and thermal comfort (Shashua-Bar, Pearlmutter, and Erell, 2011). For instance, having green spaces and urban parks in the center of the city could reduce overheating by offsetting solar radiation through evapotranspiration and air circulation(Li *et al.*, 2012). Trees, vegetation, and water bodies tend to cool the environment through shading by intercepting radiation before it reaches the surface.

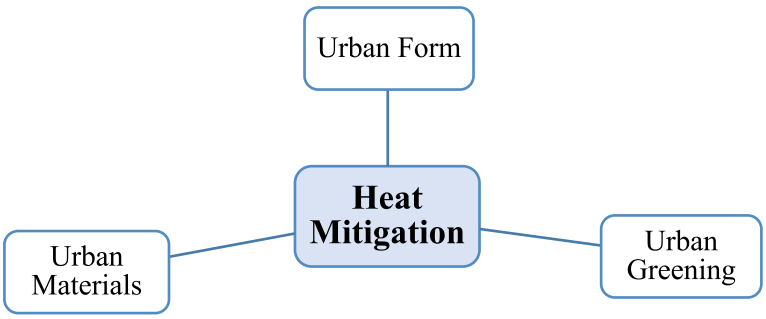

Figure 2.3 Heat mitigation strategies in cities

2.2. Green Infrastructures on Mitigating UHI

Urban Heat Island (UHI) research progresses as studies have begun to explore the cooling impacts of green infrastructure on the surrounding urban built-up areas. The use of GI in urban development and renovation is a regularly advocated technique for city adaptation policies to mitigate the UHI effect and improve thermal comfort (Degirmenci *et al.*, 2021). Green spaces such as urban park spaces typically have temperatures that are 0.5°C – 1.7°C cooler than the surrounding urban built-up areas.

2.2.1. Cooling Impacts of Urban Parks

Urban green spaces, such as urban parks have been known to have a cooling impact on their surroundings, reducing the UHI (Cao *et al.*, 2010a). Similarly, urban parks have been referred to as 'cool islands' as they have been seen to have lower surface temperatures than the surrounding built-up areas (Dousset and Gourmelon, 2003). According to this literature review, urban park is referred to as delegated open spaces with vegetation and water bodies generally located for public use (Konijnendijk *et al.*, 2013).

Urban parks can help to cool cities and reduce the urban heat island effect. Its cooling effect can spread up to 400 meters in the surrounding urban areas. Through diffusion, advection and convection, the cool air produced in the park spreads throughout the surrounding area. The intensity of cool air that spreads can vary depending on both the wind conditions and the surrounding urban layout of the park. Reduction in temperature in microclimate by urban parks is known as Park Cooling Effect (PCE). Thus, PCE can be influenced by several elements, such as the differences in climate, the park's geometric scale, vegetation coverage, vegetation type, the sky view factor (SVF) of the surrounding urban built-up area and wind conditions (Zhao *et al.*, 2011; Zhang, Gou and Lu, 2021).

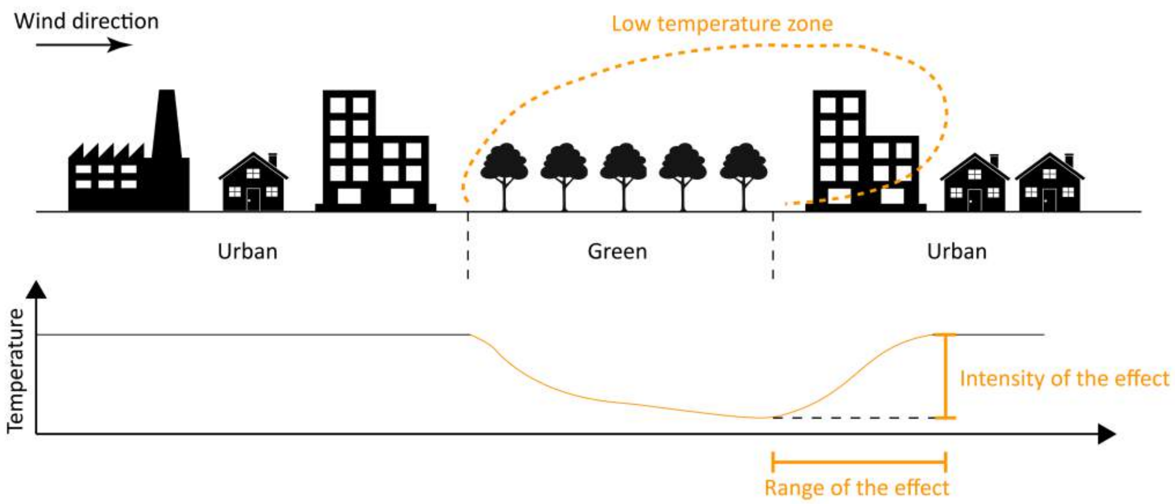

Figure 2.4 Urban Park Cooling Effect (PCE) illustration (Toparlar *et al.*, 2018).

It is important to note that the differences in climate such as the diurnal and seasonal cycles can impact an urban park's potential for cooling (Ren *et al.*, 2013). On diurnal timescales, maximum temperature drop tends to occur during the day in relation to vegetation. This is due to the exposure to direct solar radiation and shading that occurs between urban parks and urban spaces. In contrast to night-time when heat is emitted back to the atmosphere as longwave radiation, there are minimal differences in temperature between the urban parks and the urban environment. The cooling potential is strongly seen on season timescales as it reaches peak amplitude during summer. Evapotranspiration drastically reduces in autumn and winter when trees lose their leaves and canopy cover reduces (Sugawara *et al.*, 2016).

In addition to differences in climate, an urban park's geometric scale also has a great impact on its cooling potential (Id, Zinzi and Santamouris, 2017). Larger urban parks have evidently shown a more cooling impact in comparison to smaller parks. This is due to a decrease in sensible heat flux and reduced anthropogenic heat sources. However, prevailing wind conditions are also an important factor contributing to the cooling effect. Thus, cooling potential increases under stronger wind condition compared to calm conditions. Therefore, buildings surrounding urban parks should be designed to maximize ventilation.

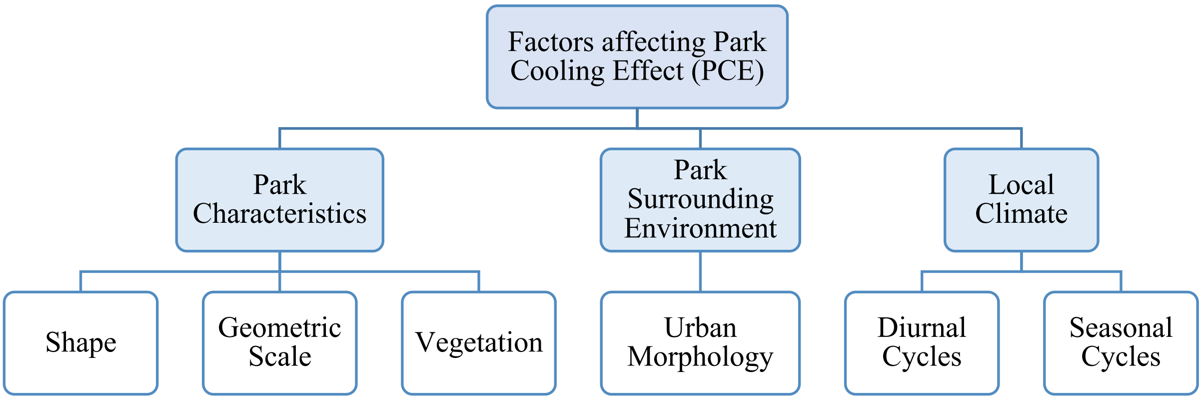

Figure 2.5 Factors affecting Park Cooling Effect (PCE)

Like the geometric scale, the shape of an urban park also influences its cooling potential. Research has shown that parks with regular shapes such as square-shaped or circular-shaped exhibit higher cooling efficiency. However, its cooling efficiency drops as the shapes become more complex (Yu *et al.*, 2017a). Furthermore, the cooling efficiency of urban parks is maximized when the shape of the park is in regular polygons in contrast to when it is in a linear shape. This is because linear parks are inclined to the invasion of heat from the surrounding areas and therefore show less difference in temperature reduction. However, urban parks of polygonal shape tend to trap cool air more efficiently through small trees and shrubs while preserving a great temperature difference (Park *et al.*, 2017).

Another fundamental factor that influences the park's cooling effect is the arrangement and type of vegetation within the urban park. Due to its evaporation characteristics, trees provide greater cooling potential compared to shrubs and grass. The larger the canopy of a tree is, the larger the shading it provides (Lee, Mayer and Chen, 2016). Both canopy size and leaf area influences shade provision.

2.3. Impacts of Urban Morphology on UHI and PCE

Urban morphology or the physical form of cities is a significant determinant of its climate at the micro and local level. The cooling effect of an urban park can be influenced by the characteristics of the surrounding built-up urban area. For instance, the density of skyscrapers and high-rise buildings surrounding the park may prevent cool breezes from dissipating the city's heat (Wang and Akbari, 2016). A great number of articles also demonstrated that urban spatial patterns influence the microclimate enhancement effect of urban parks.

Some of the important factors to be considered in park cooling effects (PCE) are the Floor Area Ratio (FAR), Canyon Aspect Ratio (H/W), building density, Sky View Factor (SVF) also known as the openness to the sky and impervious surfaces (Gunawardena, Wells and Kershaw, 2017). By determining the factors that affect the park cooling effect (PCE), existing parks can be optimized, or new urban parks can be designed to maximize the PCE effectively, mitigating the impact of UHI (Geng *et al.*, 2022)

2.3.1. Local Climate Zones (LCZ)

Local Climate Zone (LCZ) classification system developed by (Stewart and Oke, 2012) has been widely used in climate and urban heat island (UHI) studies. Different urban forms can be classified using the Local Climate Zone (LCZ) systematic scheme to identify local warming effects of urban development. LCZ consists of 10 built type classes and 7 natural land cover type classes. These are composed of 4 different properties such as the height of the buildings, the density which also reflects the compactness of the structures, land cover and the thermal properties of the structures. Hence, it is suitable for UHI studies and temperature conditions that link to the changing of urban landscape and its properties.

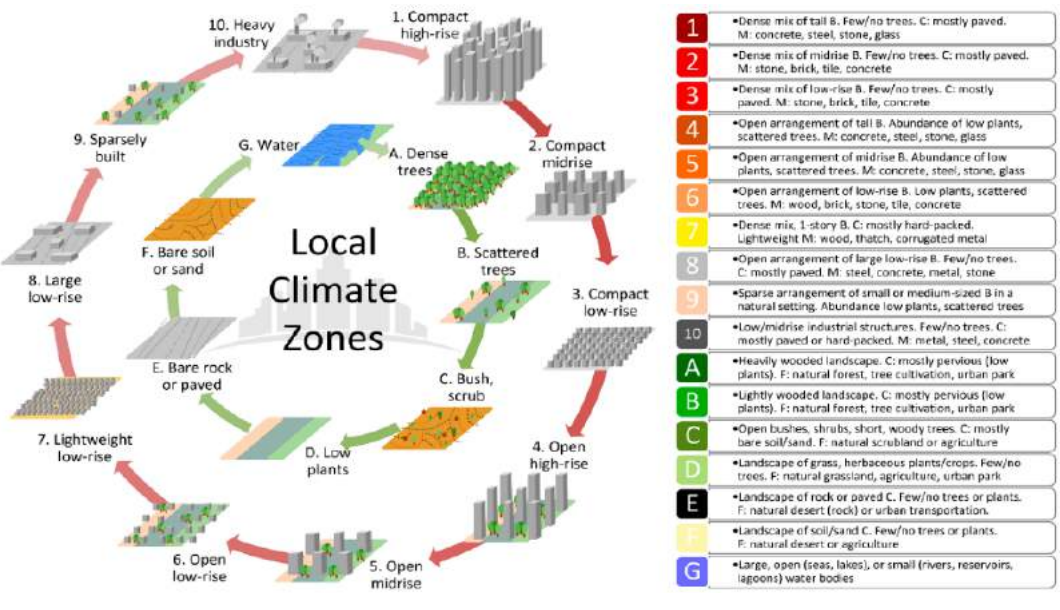

Figure 2.6 LCZ Classification

For instance, a study in Taipei, Taiwan (Chen *et al.*, 2019) and in Islamabad, Pakistan (Aslam, Rana and Bhatti, 2021) used the LCZ method for mapping temperature changes in a rapidly evolving urban environment. At a local scale LCZ has become an effective method for studying urban forms and climate. By taking into account different factors like urban structure, texture and configuration LCZ maps can be used to make new development policies.

2.4. Research & Knowledge Gaps

Cities can achieve efficiencies in their efforts to mitigate the risks associated with excessive heat if the cooling effects of restricted park spaces are used. As a result, it is vital to comprehend the impact of park characteristics on their cooling effects. Many studies have been done to examine the cooling benefits of urban parks by calculating the cooling effect of parks, identifying the main impact elements, figuring out the ideal park size, and planning and developing urban parks. The park cooling effect, which describes how much parks lower local temperatures, is not just present inside parks but is also detectable to some extent in the area immediately around parks. Several studies have shown the links of cooling effects of urban parks to the park characteristics. Although various studies have been conducted to explore the influence of urban morphology on the ecological impacts of urban parks, they are not sufficiently in-depth.

Currently, there are few studies that examine the structure of urban parks based on urban form hence a discussion on the equitable distribution of urban parks based on urban spatial morphology is essential and will help to promote a fairer and more sustainable urban planning strategy.

There are still gaps to be filled in comparing the Park Cooling Intensity (PCI) to various urban morphology. The purpose of this study is to highlight the temperature difference between an urban park and its surrounding urban area during summer using remote sensing to evaluate the potential cooling. The difference in temperature is quantified based on the variation in the urban form surrounding the urban parks.

CHAPTER 3. METHODOLOGY

3.1. Research Philosophy and Approach

According to the research onion developed by (Saunders, Lewis and Thornhill, 2019), this study involves a combination of positivism and interpretivism research philosophy. Although it focuses mainly on the link between the urban form and urban parks, positivism was considered as the main research philosophy.

The research also adopts deductive and abductive approach since the existing theory on UHI and green areas is used to construct and test the hypothesis on their relationship and further develop a framework for urban planning based on empirical knowledge. At the same time, both quantitative and qualitative are adopted throughout the research. It utilizes GIS based spatial analysis and statistical analysis techniques.

3.1.1. Research Framework

This research is quantitative by design and uses combination of GIS based spatial analysis and statistical analysis technique. Fig. 3.1 gives an overview research process taken in this study. To achieve the aim and objectives of this study, the research includes five main steps:

1. Literature review and data acquisition
2. Data Processing
3. Spatial Analysis
4. Statistical Analysis (Correlation analysis)

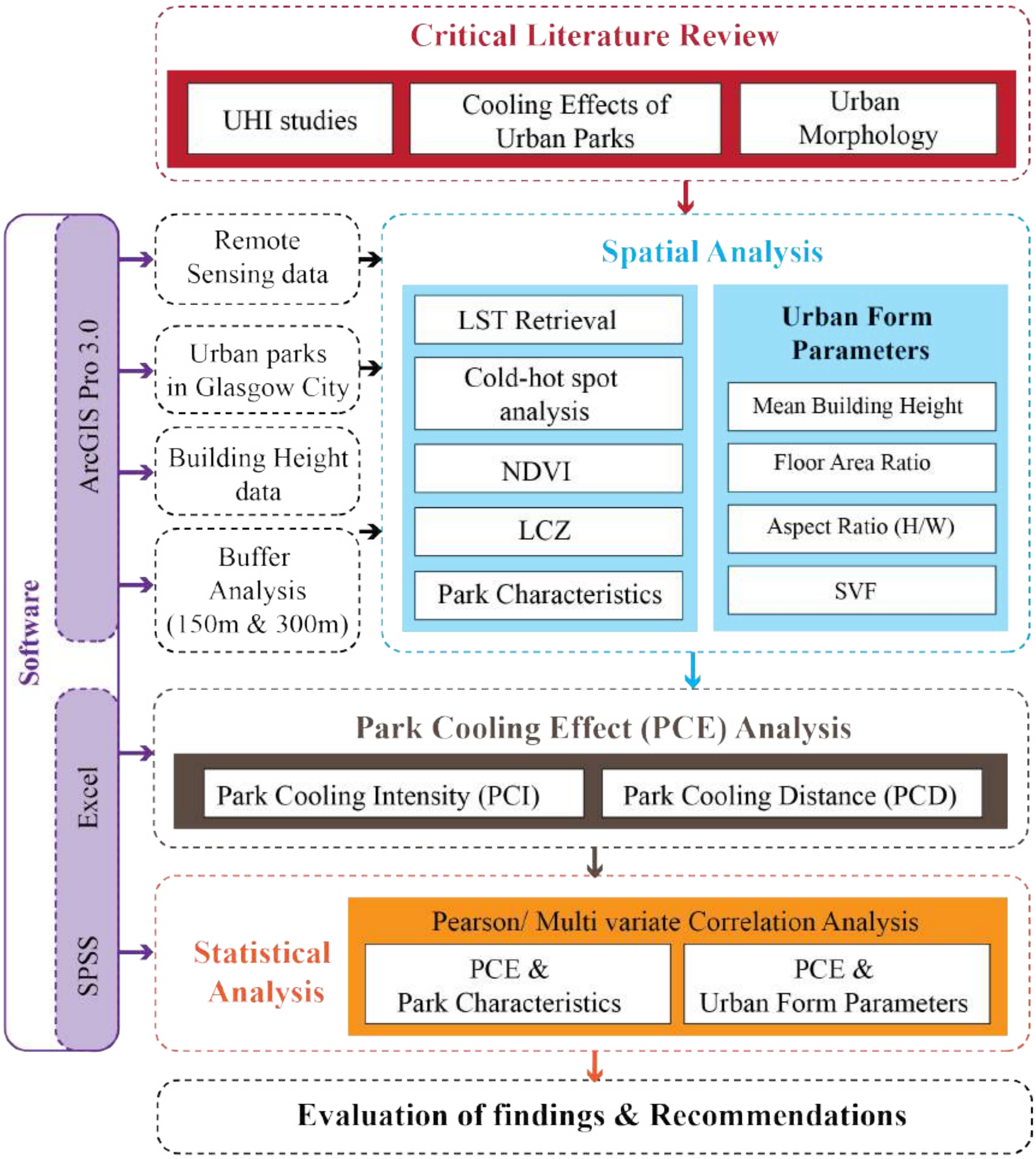

Figure 3.1 Research Framework and methodology in this study

3.2. Study Area and its Climate Conditions

Glasgow is in the West Central of Scotland, on the banks of River Clyde. It is the most populated city in Scotland and the third most populated in the United Kingdom. Glasgow City is geographically located between 55.8642° N and 4.2518° W with a total surface area of 176.4 square kilometres.

According to the census done in 2021, Glasgow City has a population of 635,130 (*statistics.gov.scot | Glasgow City*, no date). Glasgow's climate is classified as oceanic according to the Köppen-Geiger climate classification (Peel, Finlayson and Mcmahon, 2007). Glasgow has an annual average temperature of 9.6°C with a minimum temperature of 4.3°C in December and a maximum temperature of 15.9°C in July according to the daily mean temperature of 2021(Met Office).

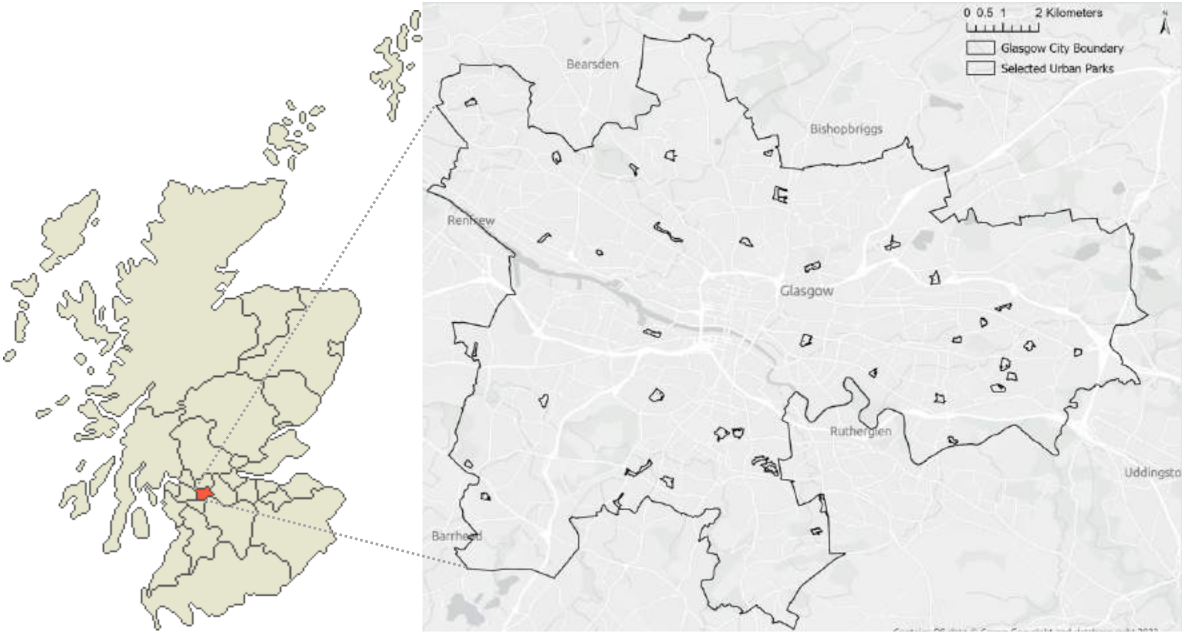

Figure 3.2 Glasgow City Map. Source: Google

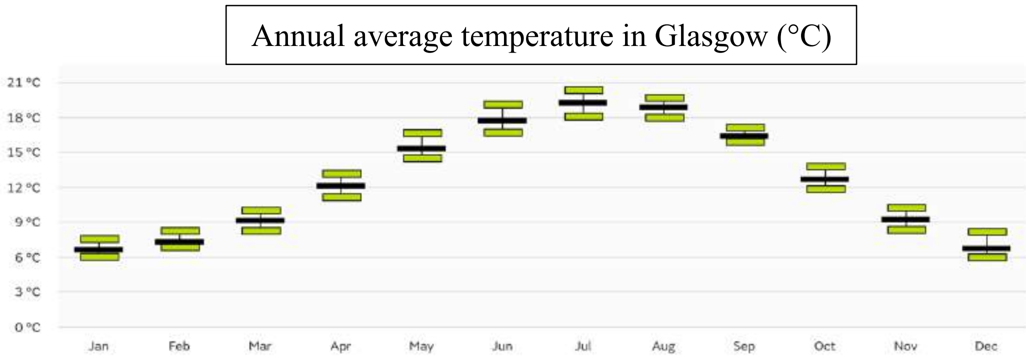

Figure 3.3 Monthly average temperature of Glasgow, Bishopton Station (UK Met Office, 2020)

Westerly winds blow across the city mostly from the west, southwest and south shown in Fig 3.4 (a). The wind is also strongest in winter and early spring and is lightest in summer as illustrated in Fig 3.4 (b).

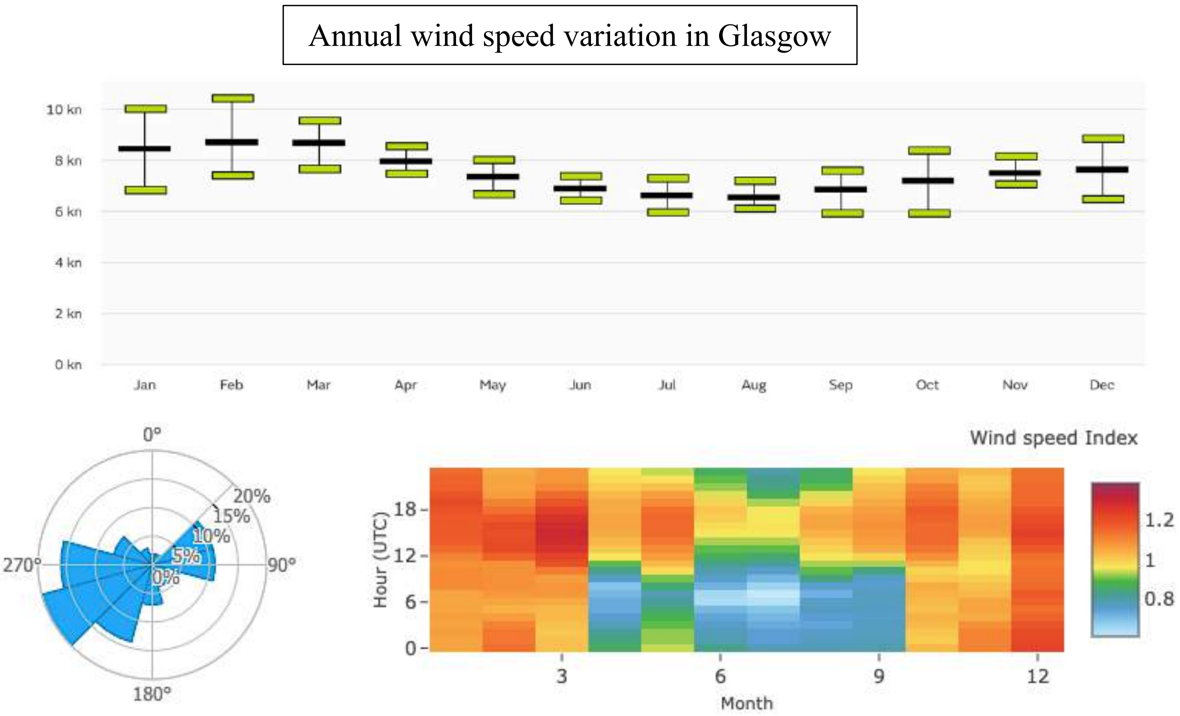

Figure 3.4 (a) Annual wind speed variation (Met Office, 2020) (b) Average wind speed rose at 10m (c) Wind speed variability, Hours vs Monthly (Source: Global Wind Atlas)

3.3. Data Collection

Table 3.1 shows a summary of the data used and collected in this study. A short description of its application is also provided in the table.

Table 3.1 Summary of the data used in this study.

	Data	Format	Provider	Date	Application
Spatial Analysis	Landsat 8 OLI_TIRS 30m Spatial Resolution	Raster (.tiff)	USGS Earth Explorer https://earthexplorer.usgs.gov/	2023	Land Surface Temperature (LST) & Normalized Difference Vegetation Index (NDVI) Retrieval
	OS Master map	Vector (.shp)	EDINA Digimap Ordnance Survey Service	2022	Street and road dimensions, Building outlines
	Land Use Data	Geopackage (.gpkg)	Urban Atlas	2018	
	LCZ	Shape file	Zala	2020	LCZ Classification, Aspect Ratio (AR),

					Sky View Factor (SVF)
	Building Height, Building Area & Road Network	Shapefile	Digimap: Ordnance Survey	2023	Mean Building Height (MBH), Floor Area Ratio (FAR)
	LiDAR Digital Surface Model (DSM)	Raster (.asc)	UBDC and Airbus Defence and Space Ltd	2022	Counter checking with building height
	LiDAR Digital Terrain Model (DTM)	Raster (.asc)	UBDC and Airbus Defence and Space Ltd	2022	
Climate	Met Office Hourly Observations Data 2018 – 2022 (Meteorological Data)	Excel (.csv)	UBDC	2022	Mean Temperature, Wind Direction, Wind Speed, Relative Humidity, and Weather Type in Glasgow from 2018 – 2022
Green Spaces	Green Spaces in Glasgow City PAN 65	Package Layer (.lpk)	Glasgow City Council	-	Urban parks selection

3.4. Land Surface Temperature (LST) Retrieval

In this study, Landsat TIRS and OLI data were used to estimate the Land Surface Temperature (LST) and NDVI variation of Glasgow City. Land Surface Temperature (LST) refers to the Earth's surface temperature measured by satellite or ground-based sensors.

Landsat 8 images were obtained from the United States Geological Survey (USGS) with cloudiness of not more than 5% to retrieve the LST. The hottest months of the year in Glasgow are from June, July and August which were used to capture the images. The satellite image was taken in 2022.

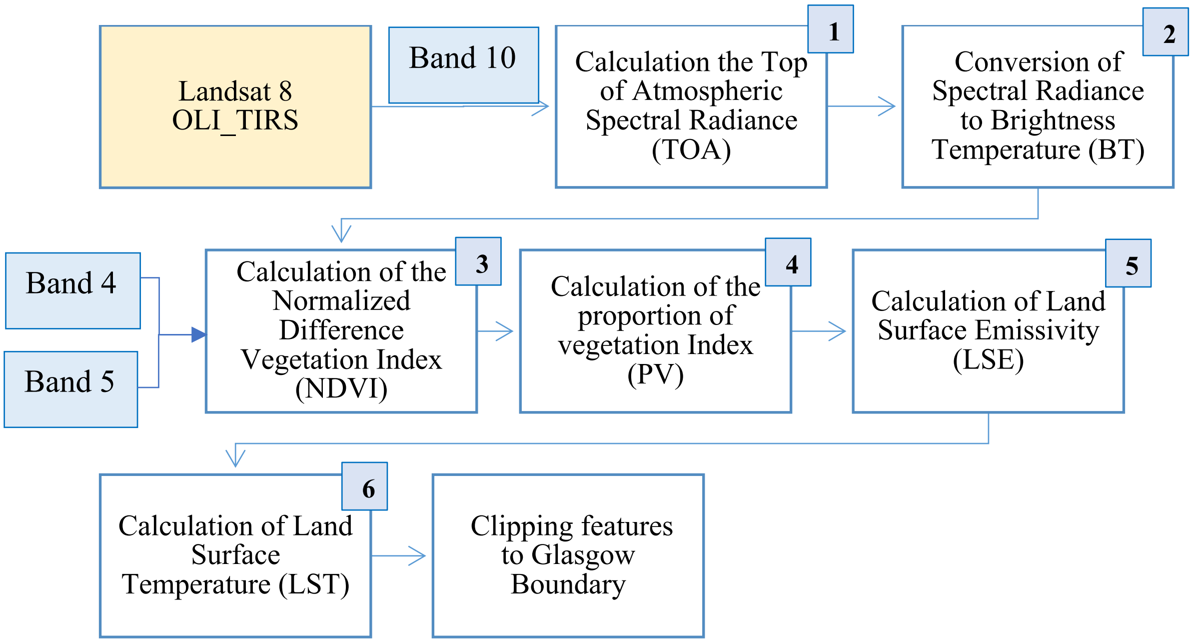

Figure 3.5 Steps used for the retrieval of LST in ArcGIS Pro 3.0

The methodology used in this study was adapted from research done by (Emmanuel *et al.*, 2023a). The steps in calculating the LST and NDVI were as follows:

Step 1: Calculating the Top of Atmospheric Spectral Radiance (TOA)

TOA is measured by Watts/(m2.Sr.μM), therefore:

$$TOA\ (L\lambda) = ML\ \times\ Qcal + AL \tag{1}$$

TOA(Lλ) = 3.3420E-04 * "

LC08_L2SP_205021_20220604_20220610_02_T1_ST_B10.TIF" + 0.10000

Table 3.2 Metadata for Satellite images used to obtain TOA

Parameter	The description on Landsat 8	Values
($L\lambda$)	Top of Atmospheric Spectral Radiance	-
ML	Radiance Multiplicative Band	3.3420E-04
Qcal	Quantized and calibrated standard product pixel values of Band 10	-
Al	Radiance Add Band 10	0.10000

Step 2: conversion of spectral radiance to Brightness Temperature (BT)

This was done using the thermal constants values acquired from the metadata file.
Converts Kelvin to Celsius using this formula:

$$BT = \frac{K2}{\ln\left(\frac{K1}{L\lambda} + 1\right)} \tag{2}$$

Table 3.3 Metadata from satellite images used to obtain BT

Parameter	The description on Landsat 8	Values
BT	Top of Atmosphere Brightness Temperature (℃)	
L$\boldsymbol{\lambda}$	Top of Atmospheric Spectral Radiance	
K1	Constant Band 10	774.8853
K2	Constant Band 10	1321.0789

Step 3: calculating the Normalized Difference Vegetation Index (NDVI)

This was done using the formula below:

$$NDVI = \frac{NIR(Band\ 5) - Red\ (Band\ 4)}{NIR(Band\ 5) + Red(Band\ 4)} \tag{3}$$

NDVI = Float (Band 5 – Band 4) / Float (Band 5 + Band 4)

Table 3.4 Metadata from Satellite Images to obtain NDVI

Parameter	Description
NIR – Near Infrared	DN values of Band 5
RED	DN values of Band 4

Step 4: Calculating the proportion of vegetation Index (PV)

PV is calculated to estimate the land surface emissivity using the formula:

$$PV = \left(\frac{NDVI - NDVImin}{NDVImax - NDVImin}\right)^2 \tag{4}$$

Table 3.5 Values used to calculate the Proportion of Vegetation Index

Parameter	Description	Values
Pv	Proportion of Vegetation Index	
NDVI	Normalized Difference Vegetation Index	
NDVImin	Min value of generated NDVI	- 0.251366
NDVImax	The max value of generated NDVI	0.982903

Step 5: Calculating Land Surface Emissivity (LSE) (ε)

$$\varepsilon = 0.004 * \text{Pv} + 0.986 \quad (5)$$

Table 3.6 Values used to calculate the Land Surface Emissivity (LSE) (ε)

Parameter	Description	Values
$\boldsymbol{\varepsilon}$	Land Surface Emissivity	
		0.004
Pv	Proportion of Vegetation	
	Correction value of the equation	0.986

Step 6: Calculating the Land Surface Temperature (LST)

LST is calculated using BT (Brightness Temperature), NDVI (Normalized Difference Vegetation Index), and LSE (Land Surface Emissivity) values acquired from the previous calculations.

$$T_s = \frac{TB}{1 + \left(\lambda \times \frac{TB}{\rho}\right) \times \ln(\varepsilon)} \quad (6)$$

$$\rho = h\frac{c}{\sigma} \quad (7)$$

Table 3.7 Values used to calculate the Land Surface Temperature (LST)

Parameter	Description	Values

BT	Top of Atmosphere Brightness Temperature	
$\boldsymbol{\lambda}$	Wavelength – Emitted Radiance	10.895
$\boldsymbol{\varepsilon}$	Land Surface Emissivity	
$\boldsymbol{\rho}$		1.438×10^{-2} mk
$\boldsymbol{h}$	Planks constant	6.626×10^{-34} J s
$\boldsymbol{c}$	The velocity of light	2.998×10^{8} m/s
$\boldsymbol{\sigma}$	Boltzmann constant	1.38×10^{-23} J/K

Finally, the derived Land Surface Temperature (LST) values were then converted from Kevin to degrees Celsius:

$$T°\mathrm{C} = T_s - 273.15 \tag{8}$$

3.5. Normalized Difference Vegetation Index (NDVI)

NDVI indicates the health and composition of greenery on the area of land. By using the reflectance in the RED and near-infrared (NIR) bands of the electromagnetic spectrum, NDVI can be obtained from remotely sensed images (Emmanuel et al., 2023b). NDVI is readily obtained with the LST retrieval process.

3.6. Urban Form Indicators

Urban Canopy and the scale of streets and buildings can have a significant impact on the wind patterns in an urban area affecting human thermal sensation. As a results, the urban morphology parameters such as the Local Climate zones (LCZ), Average building height (BH), Floor Area Ratio (FAR), Sky view factor (SVF) and Mean Aspect ratio (H/W).

3.6.1. Land cover & Local Climate Zone

To understand how land cover/ land use characteristics affects the local climate, the built-up area surrounding the urban parks need to be classified according to their key climate-influencing characteristics (Emmanuel and Loconsole, 2015). The LCZ mapping process used in this study was done on the World Urban Database Access Portal Tools (WUDAPT)s platform https://www.wudapt.org/. It was retrieved from Landsat 8 satellite image downloaded from USGS portal on February 27th, 2019.

LCZ classification is used to define the urban physical characteristics and their thermal load contribution. According to the LCZ framework by (Stewart and Oke, 2012) the estimated AR and SVF values vary within different LCZ classes. When LCZ class of buildings is classified as ‘compact’ the H/W value is more than 0.75, when it is ‘open’ it has a H/W value of 0.3 to 1.25 and when it is described as ‘sparse’ the H/W value is 0.1 to 0.25. Similarly, with vegetation cover the aspect ratio varies as well. ‘Compact’ in vegetation cover has a H/W value of more than 1, ‘open’ has a H/W value of 0.25 to 0.75 and ‘sparse’ has a H/W value of less than 0.25. Table 3.8 shows the LCZ zones various urban structure and landcover values.

Table 3.8 Local Climate Zones (LCZ)'s geometric values and surface cover properties (Stewart and Oke, 2012)

LCZ Classes	**Sky View Factor[a] (SVF)**	**Aspect Ratio[b] (H/W)**	**Building Surface Fraction[c] (%)**	**Impervious Surface Fraction[d] (%)**	**Pervious Surface Fraction[e] (%)**	**Height of roughness elements[f] (m)**
LCZ 1 - Compact high-rise	0.2 -0.4	>2	40 – 60	40 – 60	<10	>25
LCZ 2 - Compact mid-rise	0.3 – 0.6	0.75 – 2	40 – 70	30 – 50	<20	10 – 25
LCZ 3 - Compact low rise	0.2 - 0.6	0.75 – 1.5	40 – 70	20 – 50	<30	3 – 10
LCZ 4 - Open high-rise	0.5 – 0.7	0.75 – 1.25	20 – 40	30 – 40	30 – 40	>25
LCZ 5 - Open mid-rise	0.5 – 0.8	0.3 – 0.75	20 – 40	30 – 50	20 – 40	10 – 25
LCZ 6 - Open low-rise	0.6 – 0.9	0.3 – 0.75	20 – 40	20 – 50	30 – 60	3 – 10
LCZ 7 - Lightweight low-rise	0.2 – 0.5	1 – 2	60 – 90	<20	<30	2 – 4
LCZ 8 - Large low-rise	>0.7	0.1 – 0.3	30 - 50	40 – 50	<20	3 – 10
LCZ 9 - Sparsely built	>0.8	0.1 – 0.25	10 – 20	<20	60 – 80	3- 10
LCZ 10 - Heavy Industry	0.6 – 0.9	0.2 – 0.5	20 - 30	20 - 40	40 - 50	5 - 15
LCZ A - Dense Trees	<0.4	>1	<10	<10	>90	3 – 30

LCZ B - Scattered Trees	0.5 – 0.8	0.25 – 0.75	<10	<10	>90	3 – 15
LCZ C - Bush Scrub	0.7 – 0.9	0.25 -1	<10	<10	>90	<2
LCZ D – Low plants	>0.9	<0.1	<10	<10	>90	<1
LCZ E – Bare rock or paved	>0.9	<0.1	<10	<90	>10	<0.25
LCZ F – Bare soil or sand	>0.9	<0.1	<10	<10	>90	<0.25
LCZ G – Water	0.9	<0.1	<10	<10	>90	-

a Ratio of the amount of sky hemisphere visible from ground level to that of an unobstructed hemisphere
b Mean height-to-width ratio of street canyons (LCZs 1–7), building spacing (LCZs 8–10), and tree spacing (LCZs A–G)
c Ratio of building plan area to total plan area (%)
d Ratio of impervious plan area (paved, rock) to total plan area (%)
e Ratio of pervious plan area (bare soil, vegetation, water) to total plan area (%)
f Geometric average of building heights (LCZs 1–10) and tree/plant heights (LCZs A–F) (m)
g Davenport et al.'s (2000) classification of effective terrain roughness (z0) for city and country landscapes.

In this study, LCZ scheme is used to analyse the influence of urban form on PCE effect of urban parks. Additionally, the average values of LCZ classes depicted on Table 3.8 will be used to examine the surrounding urban morphology of urban parks.

3.6.2. Urban Morphological Parameters

Apart from LCZ classification, this study used various urban morphology parameters which include:

i. **Mean Building Height (MBH):**

   The average building height is an important parameter for calculating aerodynamic properties in urban areas, such as zero-displacement and roughness length. Table 3.8 shows the building classification method used in this study for distribution of building height analysis adopted from the LCZ framework component 1 which indicates the height of roughness features (Stewart and Oke, 2012).

   The average building heights were calculated in ArcGIS Pro from the attribute table derived from Building Heights data in Digimap Ordnance Survey (OS). Using the obtained spatial data, the spatial distribution of building height of Glasgow and selected urban parks were then mapped.

Figure 3.6 LCZ framework component 1- Height of roughness features (Stewart and Oke, 2012)

Table 3.9 Summary of building height classification.

Classification	Building Height
1) No rise	2) < 2 m
3) Low-rise	4) 2 – 10 m
5) Midrise	6) 10 – 25 m
7) Highrise	> 25 m

8)

ii. Floor Area Ratio (FAR):

9) Also called building density refers to the ratio of the total floor area of a building to the area of the lot on which it is located. FAR shows the intensity of land use that include two-dimensional and three-dimensional information. Analysing the FAR around urban parks and the temperature, the quantitative relationship between FAR and the PCI can be obtained.

10) 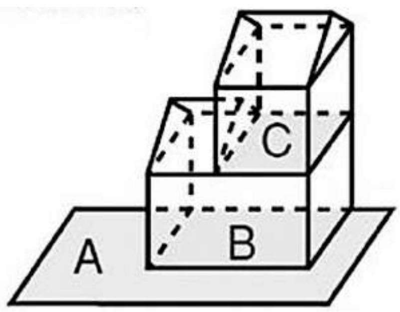

Figure 3.7 Floor Area Ratio illustration

FAR is calculated as follows:

$$FAR = \frac{Total\ Floor\ Area\ (B + C)}{Total\ area\ of\ plot\ (A)} \tag{9}$$

iii. Sky View Factor (SVF):

11) The Sky View Factor (SVF) is calculated by comparing open spaces and obstructed spaces respectively, whereas 0 indicates that the sky is not visible from a specific point in an urban canyon, while 1 means that the sky is clearly visible hence characterizing open land spaces. Therefore, high level of obstruction in an urban canyon result in lower SVF. In this study, SVF was calculated using the estimation values in LCZ framework.

12) 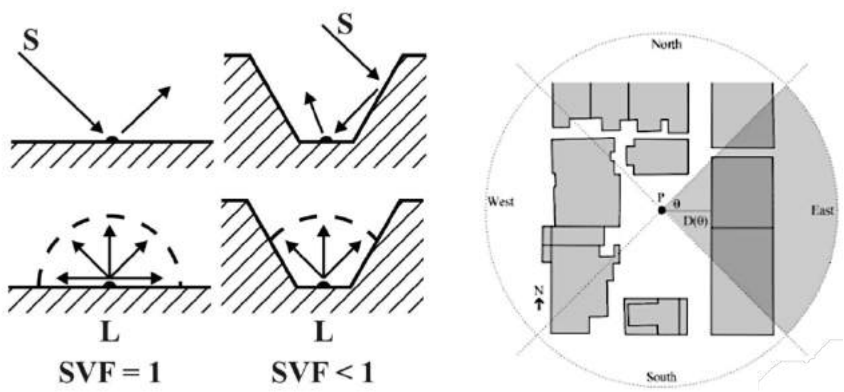

Figure 3.8 The role of surface geometry in radiation exchange. (Source:

Comparison of horizontal and convoluted surfaces. S = short-wave radiation, L = long-wave radiation. (Hämmerle et al.,2011)

$$SVF = \cos\ (\arctan(2 \times\ AR))$$

iv. Canyon Aspect ratio (H/W):

13) Also expressed by building height to street width ratio. A buildings (height-to-width) aspect ratio is a major factor in determining how much heat can be transferred from and to the environment.

14)

15) Aspect ratio is calculated as follows:

16)

17) $$\frac{H}{W} = \frac{\left(\frac{Hr}{W}+\frac{Hl}{W}\right)}{2} \qquad (10)$$

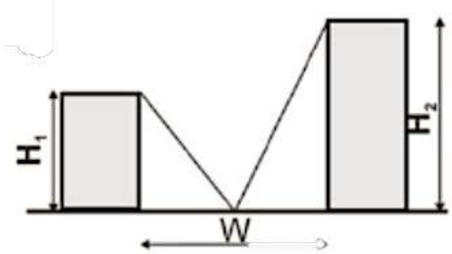

18)

Figure 3.9 Canyon Aspect ratio illustration (source:)

In this study, the aspect ratio was calculated using the LCZ framework similarly to SVF values. Street canyon can be classified into three based on the value assumed by aspect ratio. Table 3.10 shows a summary of the street canyon classification used in this study.

Table 3.10 Classification of street canyons to building aspect ratio

Aspect Ratio	**Classification**
H/W < 0.5	Avenue Canyon
H/W = 1	Regular Canyon
H/W > 2	Deep Canyon

3.7. Quantification of Cooling Effects of Urban Parks

3.7.1. Characteristics of Park Structure

In this study, three metrics have been used to investigate the how the urban park spatial arrangement can influence its cooling effect. The three metrics include: the area of the park (A), the perimeter of the park (P) and the shape index (SI) of the park. Similarly, the LCZ class of the samples of urban parks was identified as well. The area (A) and perimeter (P) of urban parks were obtained from ArcGIS from a shapefile. A Shape Index (SI) measures the relative shape complexity of parks, and it is calculated as follows (Ewers and Didham, 2007):

$$SI = \frac{P}{2 \times (\pi \times A)^{0.5}} \quad (11)$$

When SI is equal to 1, it indicates that the shape is circular. As the SI increases, the shape of the park becomes more irregular and complex.

3.7.2. Use of Buffer Analysis

Buffer analysis method was used to analyse the cooling distance of an urban surrounding within a radius of 300m from each park. The buffer zone analysis adopted from (Yu *et al.*, 2017b) is determined by the resolution of Landsat OLI_TIRS images which was 30m. 10 concentric rings of 30m in width is used as buffers to quantify the cooling effect.

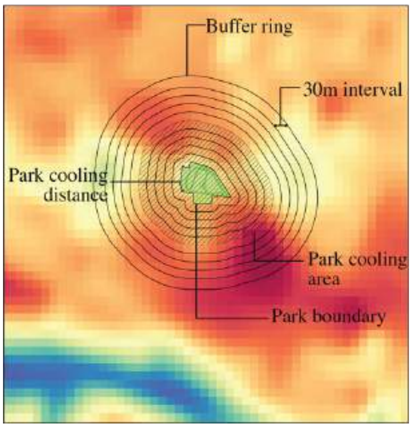

Figure 3.10 Buffer zone analysis in PCE illustration

3.7.3. Cooling effect calculation

To quantify the cooling effect of selected urban parks, this study uses the principal of the conceptual model shown in Fig. 3.12. This is done by generating a series of temperature data from the urban surroundings within the buffer zone in relation to the distance of the park. This method was used by calculated by (Lin *et al.*, 2015b) to obtain the cooling distance and the cooling intensity of green parks using remote sensing.

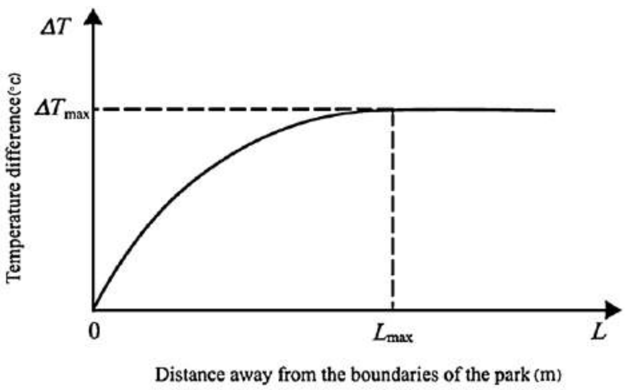

Figure 3.11 Conceptual model of the cooling effect (Source: (Lin *et al.*, 2015b))

i. Park Cooling Distance (PCD) (L_{max}): refers to the distance between a park and the limit of its cooling effect on its surroundings.

ii. Park cooling intensity (PCI) (ΔT_{max}): refers to as the difference between the temperature of the parks (T_p) and the urban areas ((T_u) which is calculated as:

$$\Delta T_{max} = T_u - T_p \tag{12}$$

3.8. Statistical Analysis

The correlation between urban morphology parameters and park cooling intensity PCI has typically been examined in two-dimensional or three-dimensional terms. Two dimensional is commonly examined as building density while three-dimensional indicator is building height (MBH), FAR, SVF and AR (H/W). In this study three-dimensional indicator is used to examine the relationship with PCI.

To understand the cooling effect of urban parks, Pearson correlation analysis between the park characteristics and PCI was conducted. In addition, curve fitting methods and multivariate regression models (MRM) were used to investigate the influence of park characteristics and urban form to PCI intensity.

MS Excel and SPSS was used to conduct all statistical analyses between PCI and its influencing factors.

CHAPTER 4. RESULTS AND ANALYSIS

4.1. Spatial Distribution of Urban Green Spaces

Pan65 Data obtained from Glasgow City Council was used to obtain the green spaces and number of urban parks present in Glasgow city. The dataset was in form of a group layer package. The selection of urban park was made in accordance with the study done by (Wang *et al.*, 2021), where it was suggested that the scale of an urban park to have the best cooling impact should be between 0.0134km2 to 0.17km2.

Therefore, the selection of urban parks in this study was done accordingly. Fig 4.1 shows the spatial distribution of the urban parks within Glasgow. To ensure a sufficient sample size requirement is met for statistical analysis 30 urban parks with a total area of around 103.5 ha, falling into various LCZ classes were therefore selected for this study. A diverse selection of urban parks throughout Glasgow city provides a great sample for analysis.

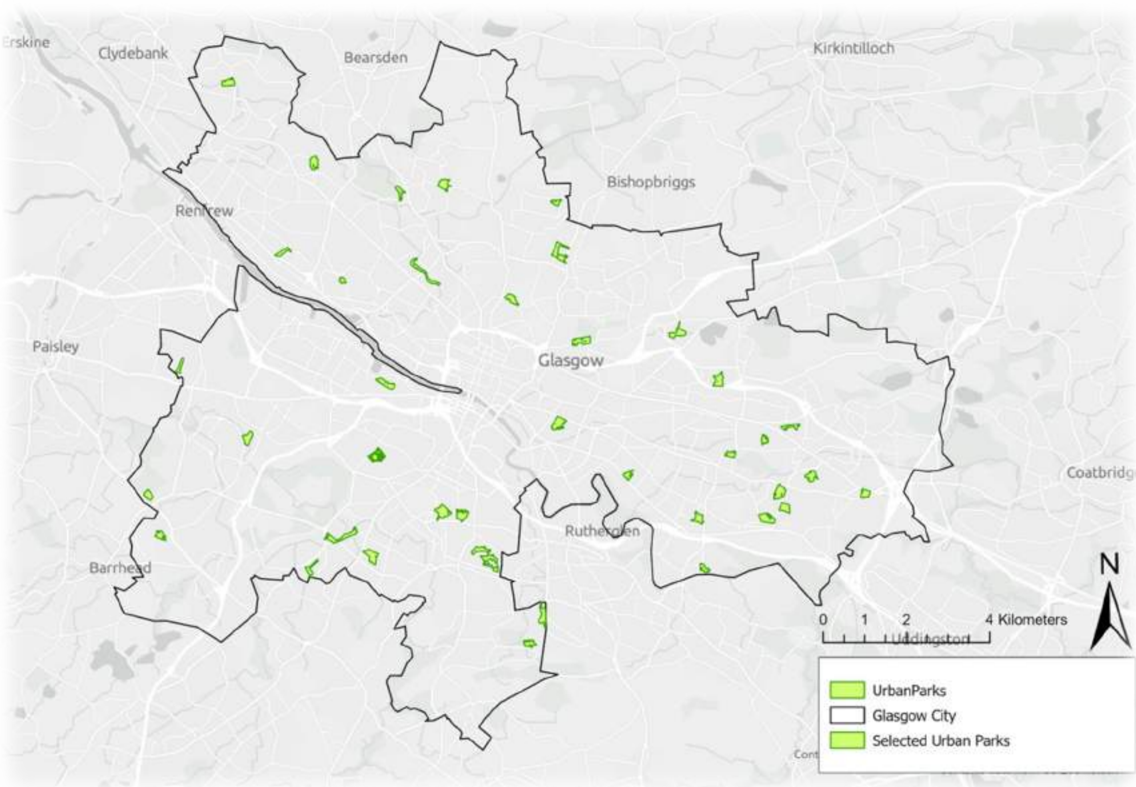

Figure 4.1 Selected urban Parks in Glasgow City

4.2. Spatial Variations of LST & NDVI

In this study, one satellite image from USGS was used to extract the Land Surface Temperature (LST) of Glasgow city. The Landsat 8 image was taken from year 2022 in 4th of June at 11am with a cloud cover of 0.20%.

Figure 4.2 shows the maximum LST in Glasgow City at 36°C and the minimum LST at 14°C on 4th June 2022. The mean LST was 25°C. According to the spatial variation of LST, high temperatures were found in built-up areas, especially where impervious surfaces were high, such as industrial and commercial areas. Moreover, the UHI effect was evidently seen in the city centre of Glasgow. North, East and South of Glasgow is seen to have low temperatures where the presence of green spaces and urban parks are located.

To analyse the greenness levels of park vegetation and the surrounding built up area, NDVI was calculated using ArcGIS. It was plotted using the same satellite imagery used for LST.

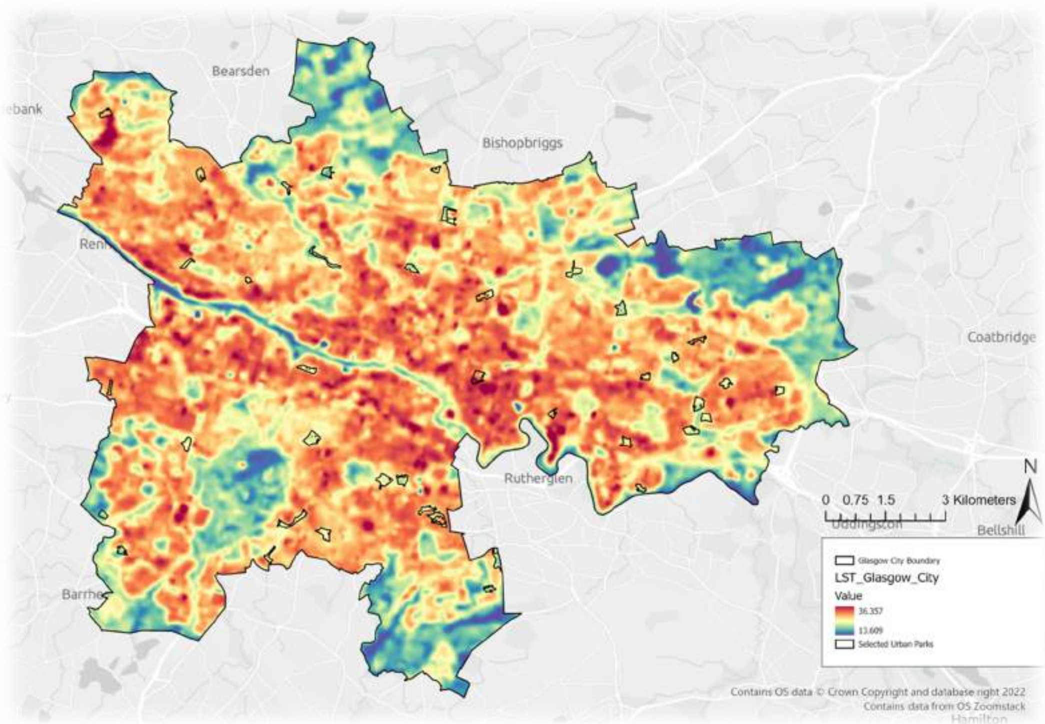

Figure 4.2 Land Surface Temperature (LST) map of Glasgow City

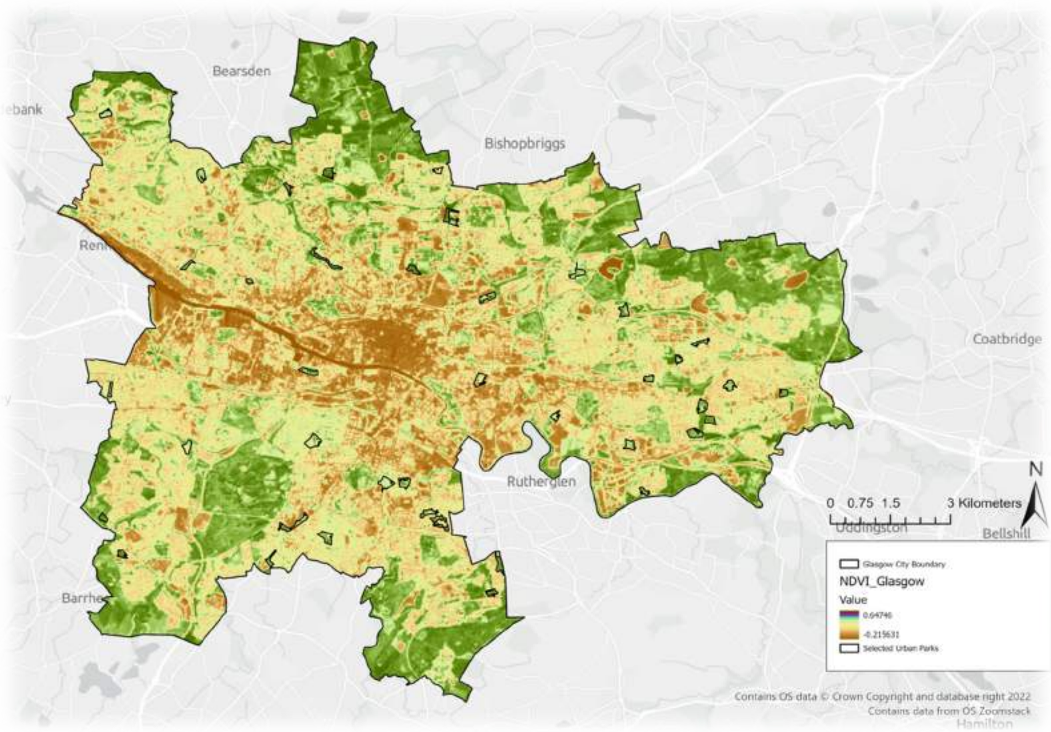

Figure 4.3 NDVI map of Glasgow City

4.2.1. Relationship Between LST and NDVI

LST shows a strong negative correlation with NDVI for Glasgow City in general. There is an increase in LST with the increase in built up areas while a decrease in LST in natural spaces, green areas, and water bodies. Thus, low LST values corresponds to high NDVI areas.

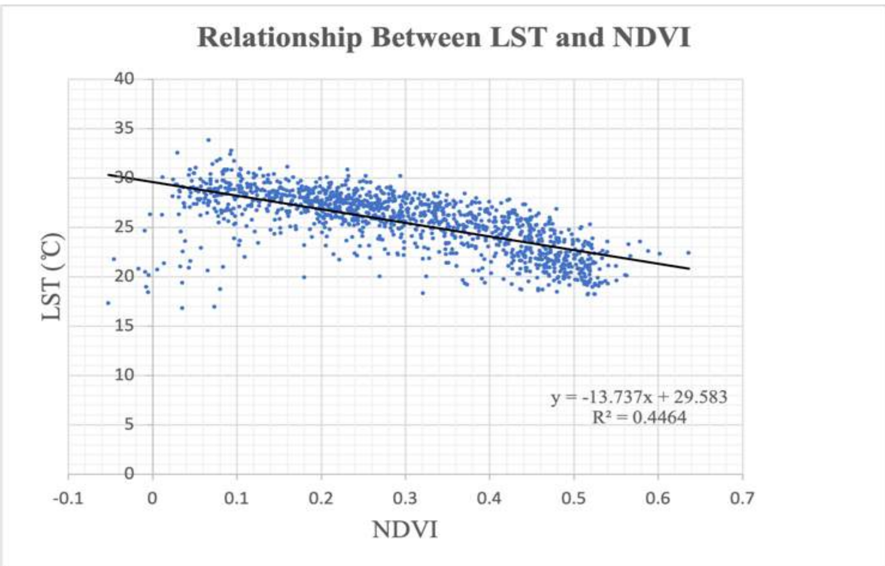

Figure 4.4 Correlation graph between LST and NDVI in Glasgow City

Table 4.1 Statistics of LST and NDVI for Glasgow City and Selected 30 Urban Parks

		LST (C)				NDVI			
		Max.	**Min.**	**Aver.**	**Std. Dev**	**Max.**	**Min.**	**Aver.**	**Std. Dev**
1	Glasgow City	36.36	13.6	25.57	2.96	0.07	-0.05	0.02	0.14
2	Ardmay Park	26.8	24.02	25.2	0.72	0.49	0.26	0.4	0.06
3	Auldhouse Park East	27.22	23.93	25.3	0.85	0.47	0.21	0.38	0.05
4	Auldhouse Park West	26.39	23.85	25.04	0.77	0.53	0.25	0.4	0.09
5	Balado Park	27.06	25.38	26.51	0.37	0.45	0.26	0.37	0.05
6	Barlanark Park	26	22.47	24.49	0.96	0.54	0.31	0.42	0.06
7	Barrachniee Park	26.35	22.26	23.91	1.2	0.49	0.32	0.42	0.05
8	Budhill Park	27.39	25.61	26.46	0.51	0.43	0.2	0.38	0.05
9	Cathkin Park	25.98	21.82	23.53	1.11	0.51	0.31	0.42	0.05
10	Cowlairs Park	26.43	21.24	23.61	1.57	0.55	0.26	0.47	0.08
11	Croftcroighn Park	24.68	21.95	22.91	0.67	0.51	0.22	0.42	0.06
12	Cross Park	26.8	24.4	25.4	0.71	0.55	0.005	0.25	0.11
13	Drumchapel Park	29.59	26.26	27.18	0.72	0.42	0.27	0.36	0.04
14	Eastfield Park	26.42	21.17	23.71	1.22	0.55	0.21	0.44	0.08
15	Festival Park	26.7	24.09	25.37	0.61	0.51	0.21	0.41	0.07
16	Fullarton Park	28.18	25.3	26.27	0.66	0.47	0.23	0.37	0.05
17	Garrowhill Park	27.0	23.1	24.7	1.1	0.50	0.29	0.39	0.04
18	Glenconner Park	27.94	24.04	26.35	1.13	0.54	0.19	0.38	0.08
19	Helenslea Park	28.71	26.54	27.32	0.67	0.47	0.13	0.32	0.08
20	Hoddam Avenue	24.9	21.9	22.74	0.76	0.54	0.18	0.43	0.09
21	James Lindsay Memorial Park	27.25	23.35	25	1.3	0.49	0.23	0.43	0.07
22	Kelhead Avenue	28.8	26.45	27.46	0.65	0.48	0.23	0.4	0.06
23	Lochar Park	27	23	24.72	1.13	0.5	0.25	0.35	0.05
24	Mansewood High Park	26.9	23.9	25.23	0.89	0.46	0.29	0.41	0.04
25	Maxwell Park	25.1	22.7	23.6	0.56	0.49	0.12	0.37	0.06
26	Milton Park	26.17	24.43	25.26	0.56	0.46	0.46	0.33	0.07
27	Mount Vernon Park	27.07	22.34	23.85	1.13	0.52	0.52	0.41	0.05
28	Newlands Park	26.3	24.4	25.3	0.55	0.53	0.24	0.41	0.06
29	Orchard Park	26.59	22.21	24.41	1.21	0.48	0.29	0.41	0.05
30	Seamill Street	25.39	21.04	23.03	1.28	0.51	0.31	0.46	0.06
31	Sherbourne Park	26.31	23.24	24.21	0.81	0.53	0.34	0.46	0.05

To deeply interpret the spatial heterogeneity of LST in Glasgow City, cold-hot spot analysis method was used.

4.2.2. Cold-Hot spot Analysis

Hot spots or Cold spots are referred to as areas which constantly show higher or lower Land Surface Temperature (LST) compared to their surrounding areas.

Optimized Hot spot Analysis tool from ArcGIS Pro 3.0 was used to calculate the Cold-Hot spot Analysis. This was done to further interpret the LST data to find statistically significant clusters. This tool analyses each feature in the context of its neighbour to determine clusters of high values (hot spot) and low values (cold spots).

Some of the selected urban parks, vegetated areas, water bodies and cold areas are seen to be overlapped indicating the cool areas while built up areas and impervious surfaces correlated with the hot spot zones. From the results, it is clear that green spaces and parks provide cooling effect in urban areas.

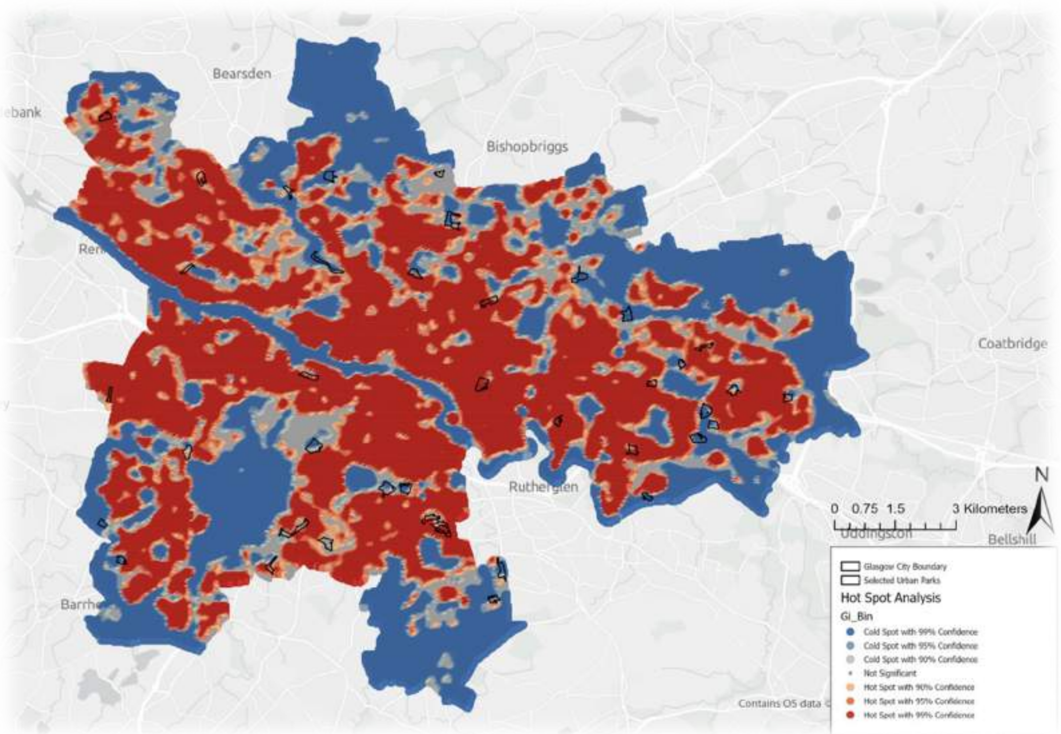

Figure 4.5 Spatial variation of cold-hot spot areas

4.3. Urban Spatial Form Analysis

4.3.1. Local Climate Zones (LCZ) & Land Use

The Local Climate Zones surrounding the urban parks were analysed to understand the urban characteristics of the built-up area. Urban parks' surrounding built up area that fall into similar LCZ classes within a residential area was considered as a criterion for further analysis.

According to the LCZ classification of Glasgow City, it reveals that the city structure includes 14 out of 17 LCZ classes. The city centre falls under LCZ 1 and 2 which is the 'compact high-rise' and 'compact midrise'. Although most of the residential area in Glasgow fall under LCZ 6 and 9 which is the 'open low-rise' and 'sparsely built' (Fig. 4.6).

The land use pattern in the selected urban park area was uniformly residential areas although the urban form varied in terms of LCZ class, and aspect ratio.

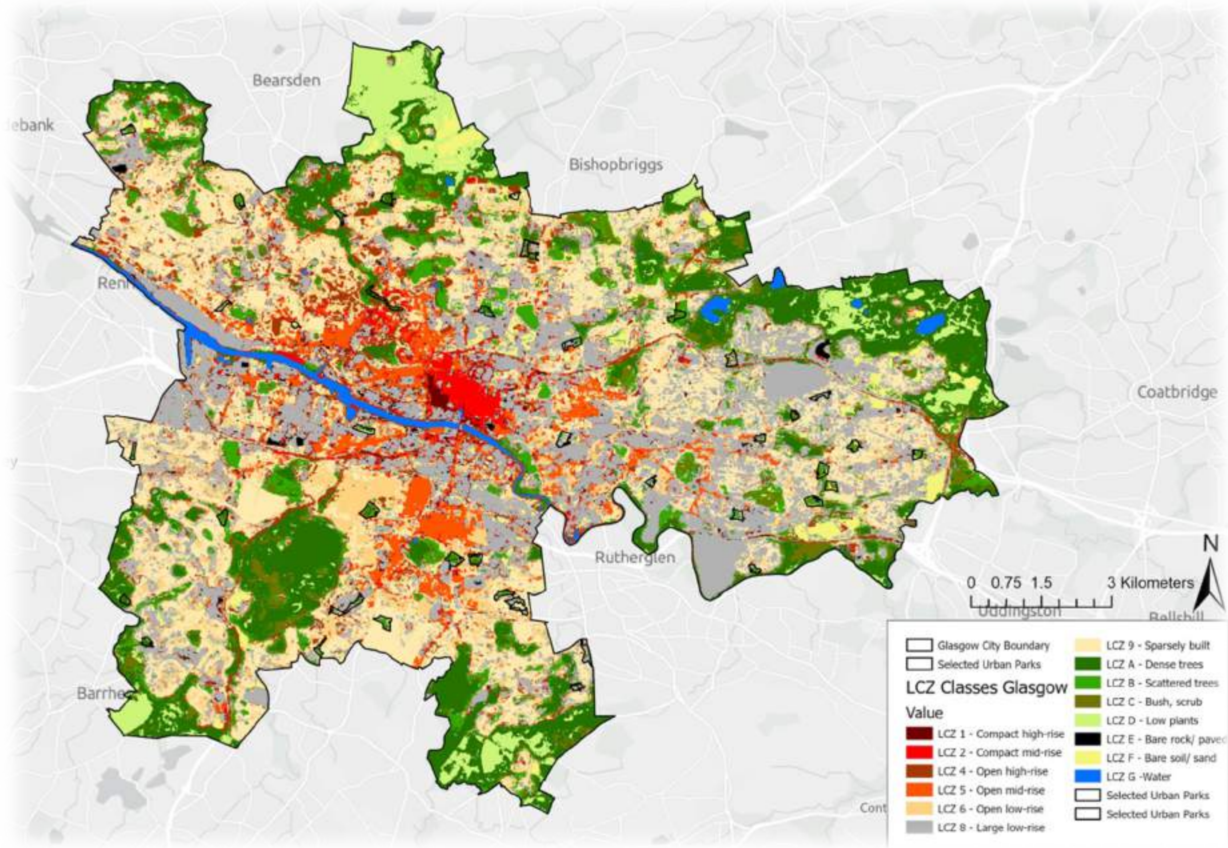

Figure 4.6 Local Climate Zone (LCZ) distribution map of Glasgow city

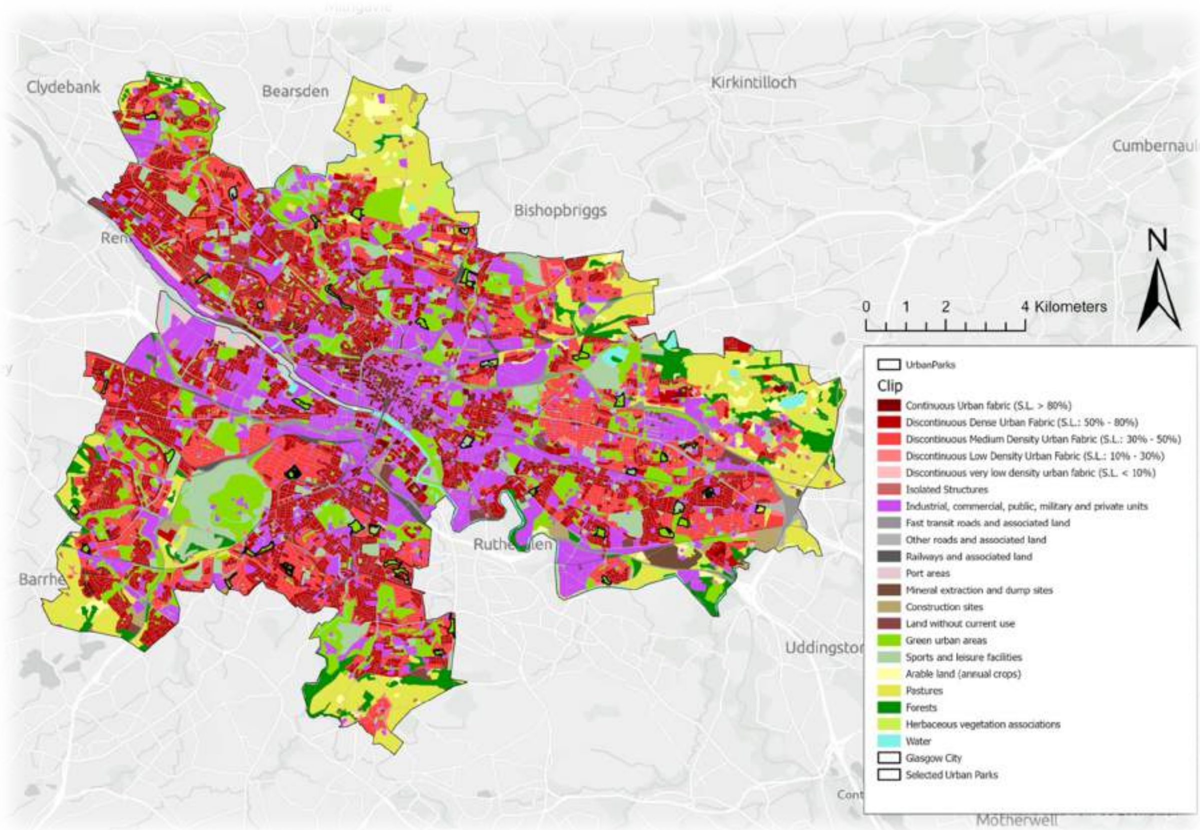

Figure 4.7 Land Use Map of Glasgow

4.3.2. Building Volume in Glasgow

Due to the obstructions from surrounding buildings, the flow trace of cool air in urban parks changes, affecting its cooling effect. Hence, the urban form surrounding urban parks, including average building height (BH), Floor Area Ratio (FAR) and other urban spatial form indicators can have an impact on its cooling effect.

The spatial distribution map of buildings in Glasgow city is shown in Fig. 4.8 and the graph is shown in Fig. 4.8. Majority of midrise and high-rise buildings are situated in the city centre of Glasgow, which also records the highest in LST, while low-rise buildings are mostly in residential areas at the outskirts of Glasgow city with low LST values. Additionally, the average building height in Glasgow is around 8 m, which shows that the urban fabric consists of low-rise buildings.

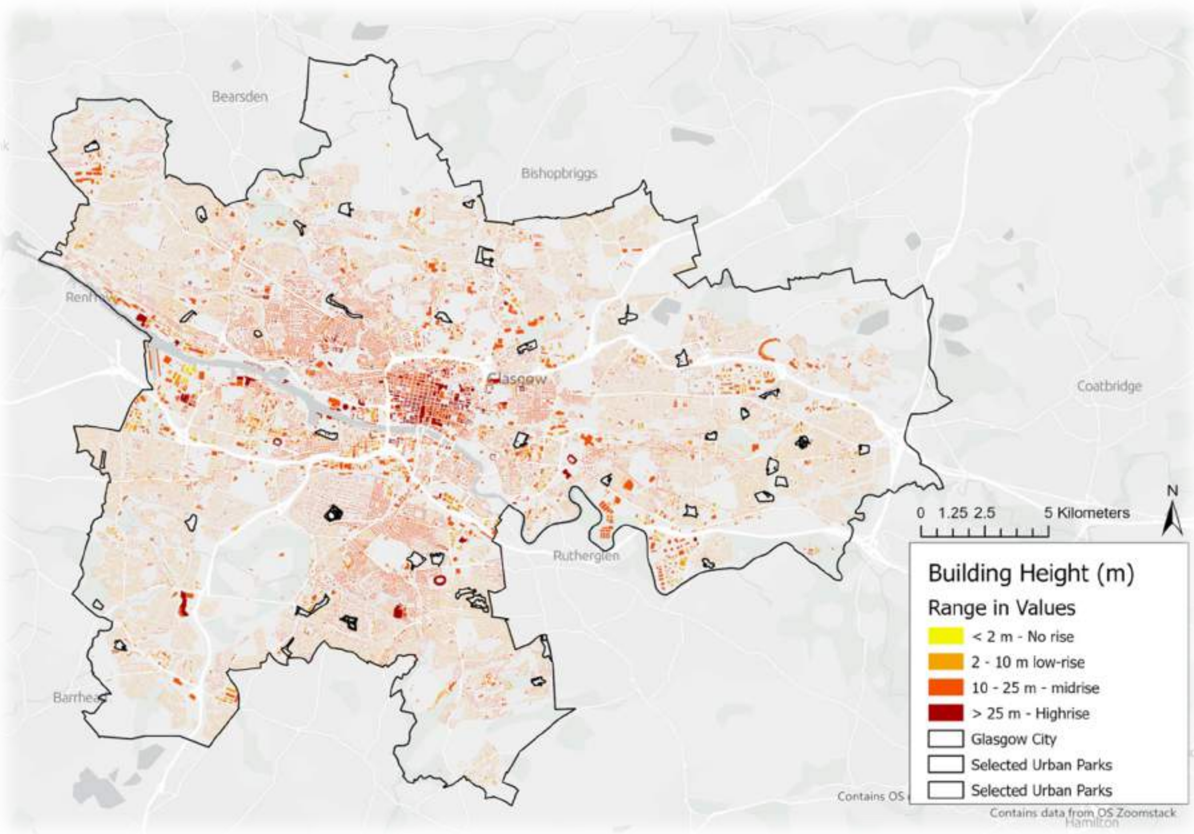

Figure 4.8 Spatial Building distribution map of Glasgow

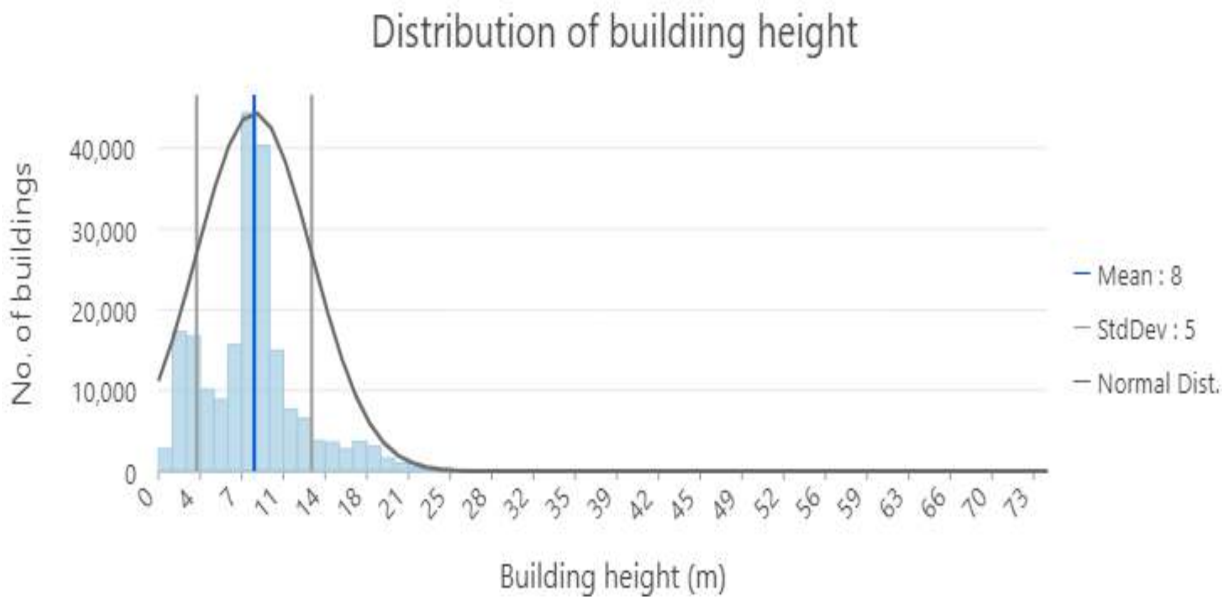

Figure 4.9 Graph of distribution of building height in Glasgow

4.4. Urban Park Characteristics

Park characteristics such as the Area (A), Perimeter (P), Shape Index (SI) and LCZ Class of 30 urban parks were obtained for further analysis.

Table 4.2 Statistics of selected urban parks

No.	**Parks name**	**Area (A) (ha)**	**Perimeter (P) (m)**	**Shape Index (SI)**	**LCZ Class**
1	Ardmay Park	3.3	1369	2.1	6,5
2	Auldhouse Park East	3.3	1388	2.2	5,6,8
3	Auldhouse Park West	2.3	1096	2.1	4,6
4	Balado Park	2.2	1419	2.7	8,9
5	Barlanark Park	2.2	968	1.8	8,9A
6	Barrachniee Park	5.5	1407	1.7	8,9
7	Budhill Park	2.4	898	1.7	8,6
8	Cathkin Park	4.4	1498	2.0	9,5
9	Cowlairs Park	3.3	1087	1.7	6,5
10	Croftcroighn Park	4.6	1246	1.6	8
11	Cross Park	1.7	606	1.31	5,6
12	Drumchapel Park	3.1	1085	1.7	9,6
13	Eastfield Park	5.8	2307	2.7	4,8
14	Festival Park	4.0	1208	1.7	8,5
15	Fullarton Park	3.6	1182	1.8	8
16	Garrowhill Park	4	3161	1.7	8,9
17	Glenconner Park	4.9	1594	2.0	8,5
18	Helenslea Park	1.9	1051	2.2	8,9,6
19	Hoddam Avenue	2.5	1360	2.4	8,9A
20	James Lindsay Memorial Park	2.9	934	1.5	8,9
21	Kelhead Avenue	1.8	887	1.9	9
22	Lochar Park	4.2	970	1.3	9,4B
23	Mansewood High Park	2.3	1332	2.5	6,9
24	Maxwell Park	6	6940	1.6	6
25	Milton Park	1.9	856	1.7	4,6
26	Mount Vernon Park	5.6	1448	1.7	8,9
27	Newlands Park	5	4631	1.7	9

28	Orchard Park	2.0	1047	2.1	9A
29	Seamill Street	2.7	1063	1.8	8,9B
30	Sherbourne Park	3.7	876	1.3	8,9

Legend		
LCZ 4 – Open high-rise	LCZ 8 – Large low-rise	LCZ A – Dense trees
LCZ 5 – Open mid-rise	LCZ 9 – Sparsely built	LCZ B – Scattered trees
LCZ 6 – Open low-rise		

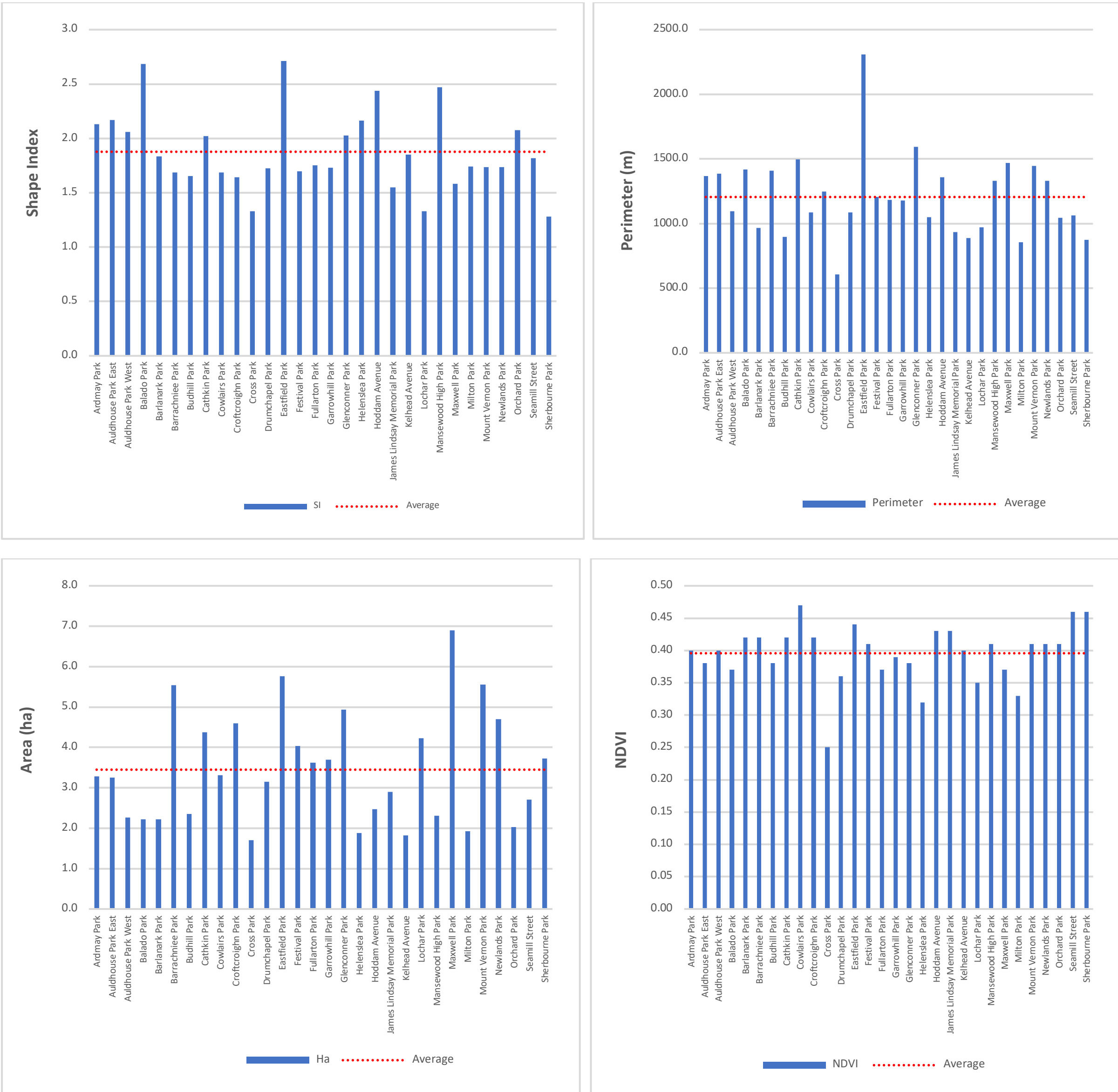

Figure 4.10 Overall results for the 30 parks (a) Shape Index (b) Perimeter (m) (c) Area (ha) (d) NDVI

4.5. Analysis of the Potential Cooling Effects (PCE) of Urban Parks

4.5.1. Use of Buffer analysis

To determine the cooling distance of the urban park, 10 buffers of 30 meters wide was used to examine thermal differences between the park and surrounding built up area. Additionally, two concentric rings of 150m and 300m were used to analyse the thermal difference and the maximum park cooling distance. The average temperature of each ring was calculated. This method was adopted from (Yu *et al.*, 2017b) where PCI is calculated as the difference between the LST of the first turning point of decline within the buffer area and the LST of the park. The parks characteristics are independent variables while PCI and PCD are dependent variables.

Table 4.3 Statistics of LST in Selected Urban Parks and the Buffer area 300 m

No.	**Park**	**Mean LST(°C) Park**	**Mean LST(°C) Buffer 150m**	**Mean LST(°C) Buffer 300m**	**ΔT(°C) 150m Buffer - Park**	**ΔT(°C) 300m Buffer - Park**	**ΔT(°C) 300m - 150m buffer**
1	Ardmay Park	25.2	27.2	27.63	2	2.43	0.43
2	Auldhouse Park East	25.3	27.31	27.24	2.01	1.94	-0.07
3	Auldhouse Park West	25.04	26.32	26.1	1.28	1.06	-0.22
4	Balado Park	26.51	26.94	27.07	0.43	0.56	0.13
5	Barlanark Park	24.49	25.39	25.56	0.9	1.07	0.17
6	Barrachniee Park	23.91	26.08	26.07	2.17	2.16	-0.01
7	Budhill Park	26.46	27.61	27.42	1.15	0.96	-0.19
8	Cathkin Park	23.53	26.37	26.65	2.84	3.12	0.28
9	Cowlairs Park	23.61	26.55	26.87	2.94	3.26	0.32
10	Croftcroighn Park	22.91	25.01	25.3	2.1	2.39	0.29
11	Cross Park	25.3	27.2	27.3	1.9	2	0.1
12	Drumchapel Park	27.18	27.49	27.14	0.31	-0.04	-0.35
13	Eastfield Park	23.71	25.7	25.82	1.99	2.11	0.12
14	Festival Park	25.37	27.54	27.28	2.17	1.91	-0.26
15	Fullarton Park	26.27	28.42	28.17	2.15	1.9	-0.25
16	Garrowhill Park	24.7	27.1	27.5	2.4	2.6	0.2
17	Glenconner Park	26.35	26.96	27.17	0.61	0.82	0.21
18	Helenslea Park	27.32	28.13	28.35	0.81	1.03	0.22
19	Hoddam Avenue	22.74	24.07	23.69	1.33	0.95	-0.38

20	James Lindsay Memorial Park	25	26.75	27.37	1.75	2.37	0.62
21	Kelhead Avenue	27.46	27.64	27.9	0.18	0.44	0.26
22	Lochar Park	24.72	26.14	26.23	1.42	1.51	0.09
23	Mansewood High Park	25.23	25.94	25.83	0.71	0.6	-0.11
24	Maxwell Park	23.7	25.7	25.9	2	2.2	0.2
25	Milton Park	25.26	25.72	25.25	0.46	-0.01	-0.47
26	Mount Vernon Park	23.85	25.32	25.53	1.47	1.68	0.21
27	Newlands Park	25.3	26.50	26.6	1.2	1.3	0.1
28	Orchard Park	24.41	25.89	25.62	1.48	1.21	-0.27
29	Seamill Street	23.03	25.92	26.23	2.89	3.2	0.31
30	Sherbourne Park	24.21	25.36	25.24	1.15	1.03	-0.12

4.6. Analysis of Parks Surrounding Urban Form

The built-up area surrounding urban parks influences its cooling effect. The cooling effect can vary if an urban park is surrounded by large water bodies, bare ground or different building heights and density. In this study, the surrounding urban form such as the MBH and FAR of the urban parks were analysed from the building height data obtained from Digimap while SVF and AR was obtained using the estimated values of LCZ classes.

The Spatial building distribution surrounding each park were analysed in a 300m buffer area. Table 4.4 shows a summary statistical analysis of the building height around 30 selected urban parks. The observation made on the urban built-up area surrounding the parks were as follows:

i. **Average Building Height (MBH)**

The mean building height among the 30 urban parks was 7.68 m. The maximum height was 11 metres which was seen around Cross Park. Cross Park showed a trend of mixed urban fabric consisting 56% of open midrise buildings with 39% low-rise buildings. The minimum height was 6 m was seen around Barrachnie, Fullarton and Mount Vernon Park.

ii. **Floor Area Ratio (FAR)**

FAR was analysed in all 30 urban parks surrounding built up area of the buffer zone to further examine the quantitative relationship between FAR and PCI. According to the statistical analysis obtained from the building data shown in Table 4.4, the FAR around the urban parks is between 0 to 8. The highest FAR was seen around Festival Park of 7.99 while the lowest was around Garrowhill park with FAR of 0.70. The mean FAR of the built-up area around all 30 urban parks was 2.31.

iii. Sky View Factor (SVF)

The average SVF of the surrounding park area was 0.753. The maximum was 0.9 seen around Newlands Park and Orchard Park, while the minimum was 0.625 around Eastfield Park.

iv. Aspect Ratio (H/W)

The average aspect ratio was 0.369 of all 30 urban parks. The maximum was 1.063 around Orchard Park while the minimum was 0.125 around Newlands Park.

Table 4.4 Summary statistical analysis of urban form parameters values obtained

No.	Park	LCZ Class	MBH (m)	FAR	SVF	AR (H/W)
1	Ardmay Park	6,5	7	1.53	0.700	0.525
2	Auldhouse Park East	5,6,8	8	2.80	0.750	0.525
3	Auldhouse Park West	4,6	8	2.41	0.675	1.013
4	Balado Park	8,9	8	7.21	0.875	0.163
5	Barlanark Park	8,9A	8	1.53	0.650	0.163
6	Barrachniee Park	8,9	6	0.97	0.875	0.163
7	Budhill Park	8,6	7	1.74	0.700	0.363
8	Cathkin Park	9,5	8	3.05	0.775	0.325
9	Cowlairs Park	6,5	8	4.09	0.733	0.613
10	Croftcroighn Park	8	8	0.82	0.650	0.200
11	Cross Park	5,6	11	3.1	0.700	0.525
12	Drumchapel Park	9,6	8	2.87	0.825	0.325
13	Eastfield Park	4,8	10	1.89	0.625	0.350
14	Festival Park	8,5	9	7.99	0.650	0.363
15	Fullarton Park	8	6	2.14	0.650	0.200
16	Garrowhill Park	8,9	6.3	0.7	0.775	0.163
17	Glenconner Park	8,5	9	2.25	0.650	0.363
18	Helenslea Park	8,9,6	8	2.18	0.767	0.425

19	Hoddam Avenue	8,9A	8	0.78	0.775	0.163
20	James Lindsay Memorial Park	8,9	7	0.82	0.775	0.163
21	Kelhead Avenue	9	8	1.86	0.900	0.125
22	Lochar Park	9,4B	8	2.86	0.750	0.813
23	Mansewood High Park	6,9	8	1.93	0.825	0.325
24	Maxwell Park	6	7	2.8	0.750	0.525
25	Milton Park	4,6	7	0.71	0.675	0.513
26	Mount Vernon Park	8,9	6	1.59	0.775	0.163
27	Newlands Park	9	7	1.7	0.900	0.125
28	Orchard Park	9A	7	1.67	0.900	1.063
29	Seamill Street		8	2.59	0.775	0.163
30	Sherbourne Park	8,9	6	0.86	0.775	0.163

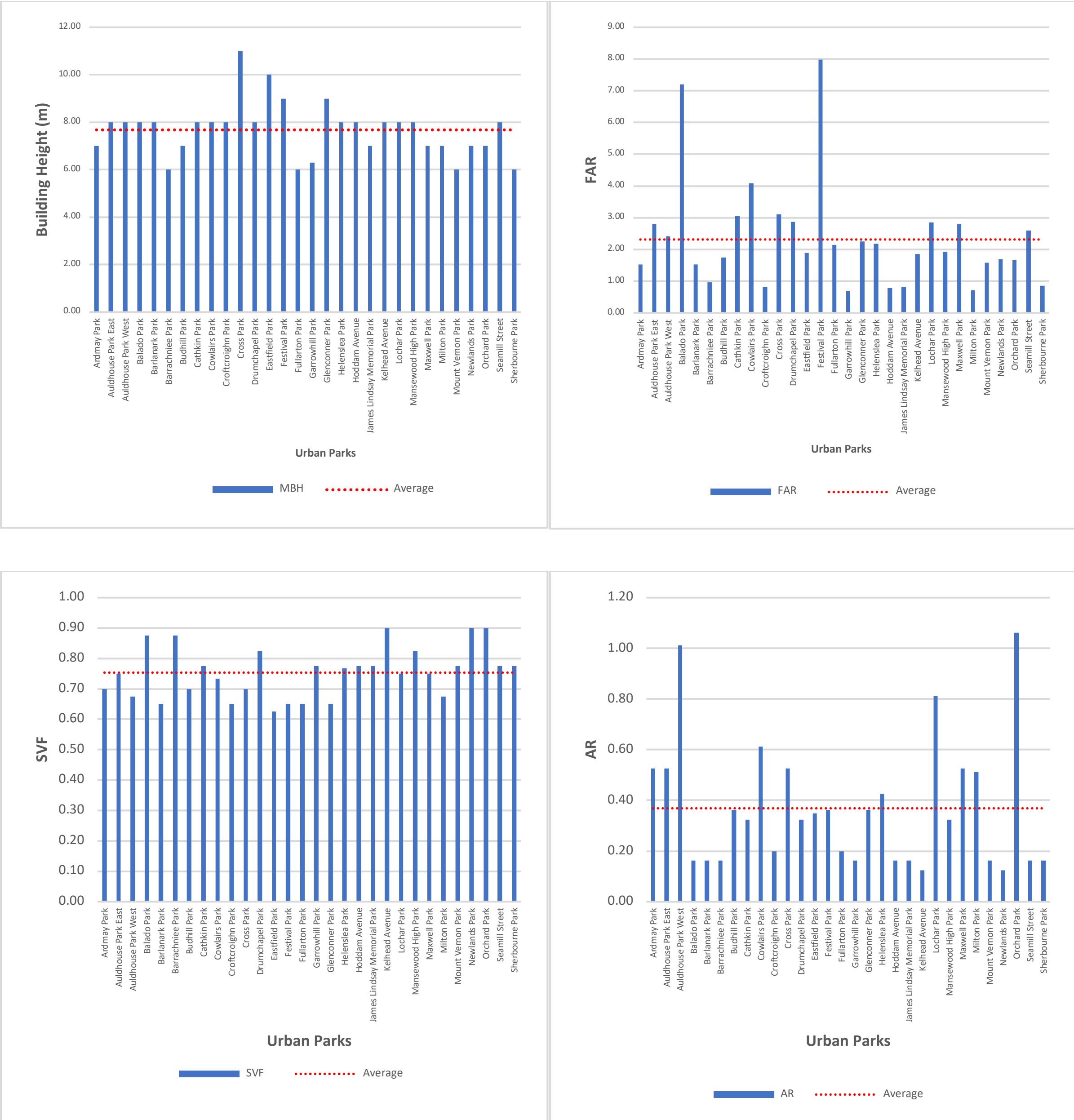

Figure 4.11 Overall results of the urban form parameters calculated for 30 parks surrounding built up areas; (a) Mean Building Height (m) (b) Floor Area Ratio (FAR) (c) Sky View Factor (SVF) (d) Aspect Ratio (H/W)

CHAPTER 5. DISCUSSION OF RESULTS AND IMPLICATIONS

This chapter highlights and evaluates this study's findings to other research studies from the field. It further discusses their practical implications for urban planning.

5.1. Park Cooling Effect (PCE) of Urban Parks

Urban parks of sizes between 1.3 ha ($0.013km^2$) to 6 ha ($0.06km^2$) in residential and mixed land use areas were considered in this study. According to the results achieved in this study, the mean LST around the buffer area of 150m and 300m and the mean LST in the 30 urban parks were significantly lower, revealing that urban parks can effectively mitigate the effects of UHI. To assess the cooling intensity of the parks and the influencing factors selected urban parks were analysed for PCE according to their park characteristics (Area, perimeter, shape index and NDVI) and urban form of the surrounding park area including the (LCZ, MBH, FAR, H/W, and SVF). Subsequently, park characteristics and urban form parameters were then correlated to PCI intensity to uncover the relationship between them. An evaluation of each parameter was then done using multivariate regression analysis.

5.1.1. Park Cooling Intensity (PCI) of Urban Parks

Park cooling Intensity (PCI) also showed as (ΔT_{max}) in Fig. 5.1 was used to assess the cooling effect of 30 urban parks in different areas of Glasgow. In this study, PCI is referred to the LST differences between the park and the surrounding urban area (Lin *et al.*, 2015c). By using two concentric rings of 150 m and 300 m buffer area was made around each park. The average LST of each park and its two rings were analysed, and their temperature difference was therefore regarded as PCI.

The average PCI was calculated for all parks using the Overlay and Statistic Analysis tools in ArcGIS Pro 3.0. The LST differences between the parks and buffer zone were calculated to examine the PCI spatial variability. It was noted that the parks were 1.6°C cooler than their surrounding built up areas. However, there was no significance difference in temperature with the average LST of Glasgow City which was 25°C. The results evidently showed that green spaces do lower the LST in urban areas.

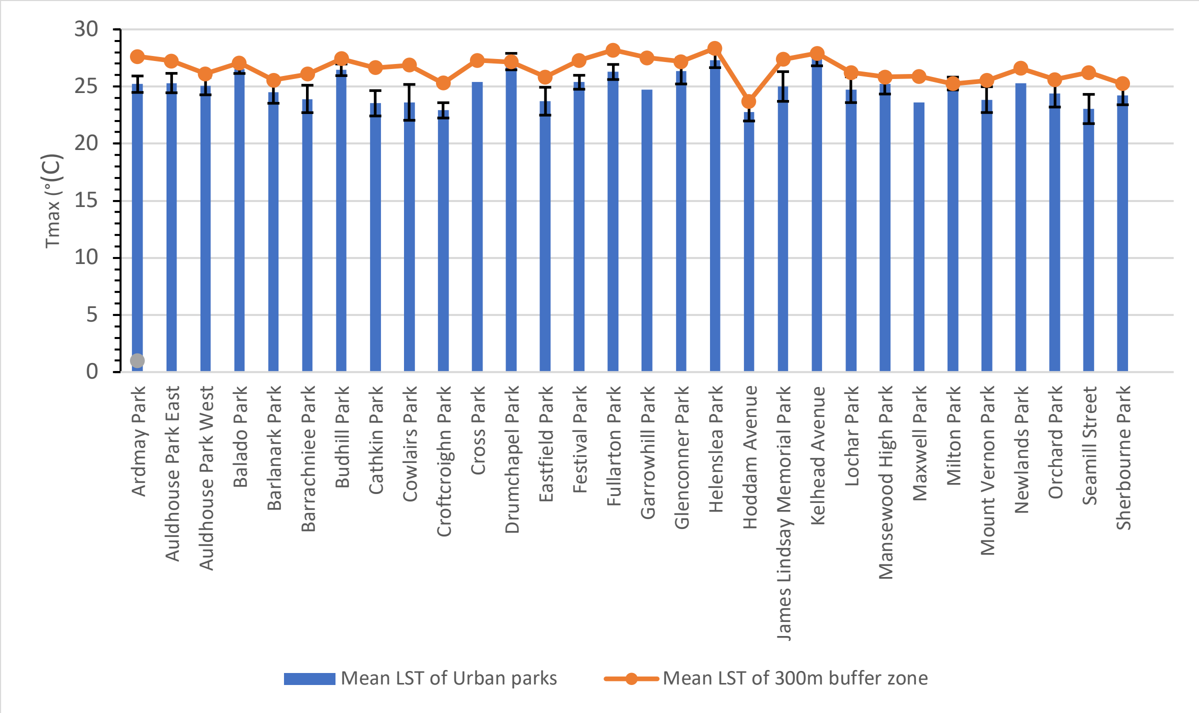

Figure 5.1 Graph of temperature difference between urban parks and the buffer zone of the surrounding built up area

Among the 30 parks, 28 parks were cooler than the surroundings whereas only 2 (Drumchapel & Milton Park) showed no significance cooling effect. The urban park with the highest cooling effect was Cowlairs Park with an area of 3.3 ha (3.26°C) and the lowest was Kelhead Avenue Park with an area of 1.8 ha (0.4°C).

5.1.2. Park Cooling Range of Urban Parks

Park Cooling Distance (PCD) also referred to as L_{max} was taken as the distance between a park and the limit of its cooling effect on its surroundings. Again, the average surface temperature in two concentric rings of 150m and 300m buffer area were analysed as shown in Fig. 5.3. The fitting results in Fig. 5.2 show the cooling distance and temperature conform to the law of cubic function. In the graphs below, the cubic polynomial curve is seen to initially increase steeply and then change gently with the increase of distance.

The point of inflection of cubic polynomial indicates the maximum influence cooling distance (L_{max}) of an urban park. L_{max} can be substituted to obtain the maximum temperature (ΔT_{max}) within the cooling range of the urban park.

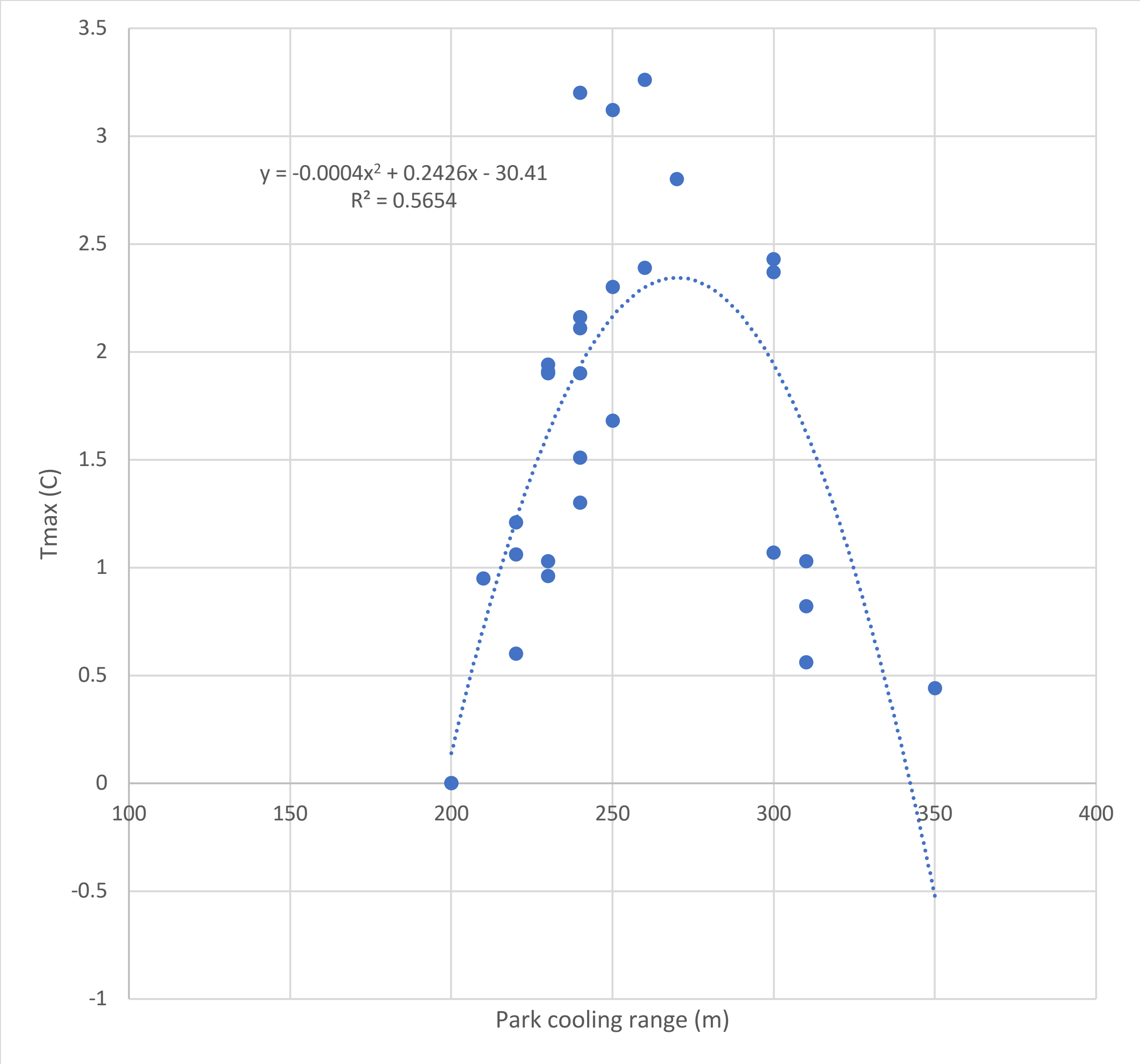

Figure 5.2 Fitting results between Tmax and Lmax

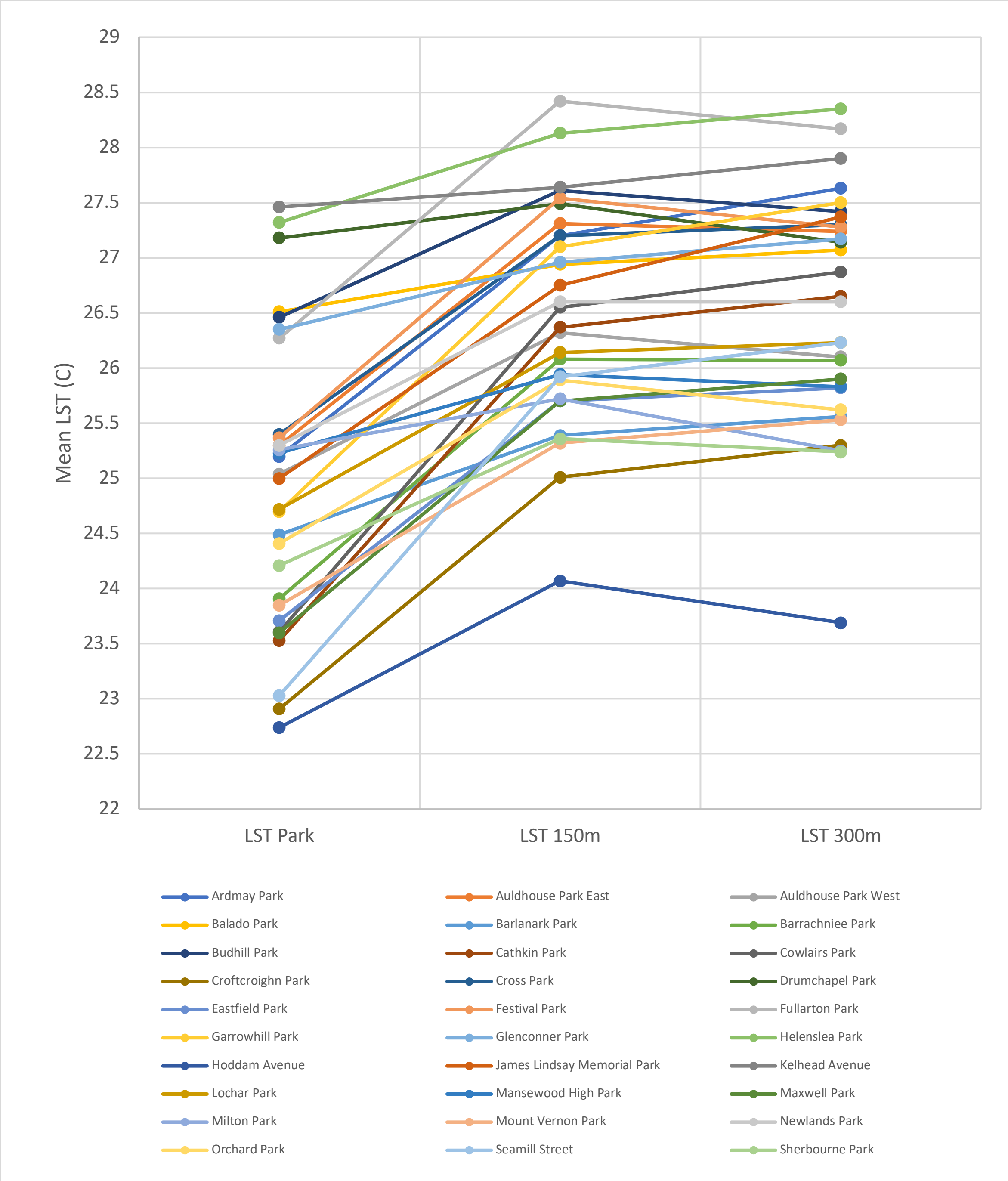

Figure 5.3 Observation graph of mean LST of urban parks and two buffer rings of 150m and 300m

In general, LST of urban parks were lower inside than in their buffer zones, although the LSTs gradually increased with the distance from the park as shown in Fig. 5.3. A sharp increase is observed within 150 m buffer zone followed by a slight decrease in temperature as it progresses.

The sample urban parks' sizes varied from 1.7 ha to 6.9 ha in area. Even though there isn't a major difference among the area and perimeter of parks, the variation of cooling distance was noticed.

5.2. Influencing Factors of Urban PCE

5.2.1. Correlation Analysis of Park Characteristics and PCI

Parks characteristics such as the area, perimeter, shape index and canopy intensity (NDVI) can have an impact on the intensity of the cooling effect. To further analyse the cooling strength, a multi variate correlation between the PCI and park characteristics were calculated. This included the area, perimeter, shape index and NDVI of the urban parks. The correlation analysis results between PCI and the independent variables are shown in Table 5.1. The R^2 coefficient of determination for the park characteristics to its PCI was 0.3416, showing that the correlation between the variables and PCI was positive. Similarly, a positive correlation was seen between the area, perimeter and NDVI of park and the PCI. However, a negative correlation was observed between the shape index and PCI. The study indicates that more vegetation can enhance the cooling performance of parks.

Table 5.1 Correlation between PCI and the park characteristics

	Park Cooling Intensity PCI	
	Pearson Correlation	Significance
Area	0.4129	0.2077
Perimeter	0.2144	0.0114
SI	-0.1899	0.0770
NDVI	0.3605	0.0944

n = 30

(a) (b)

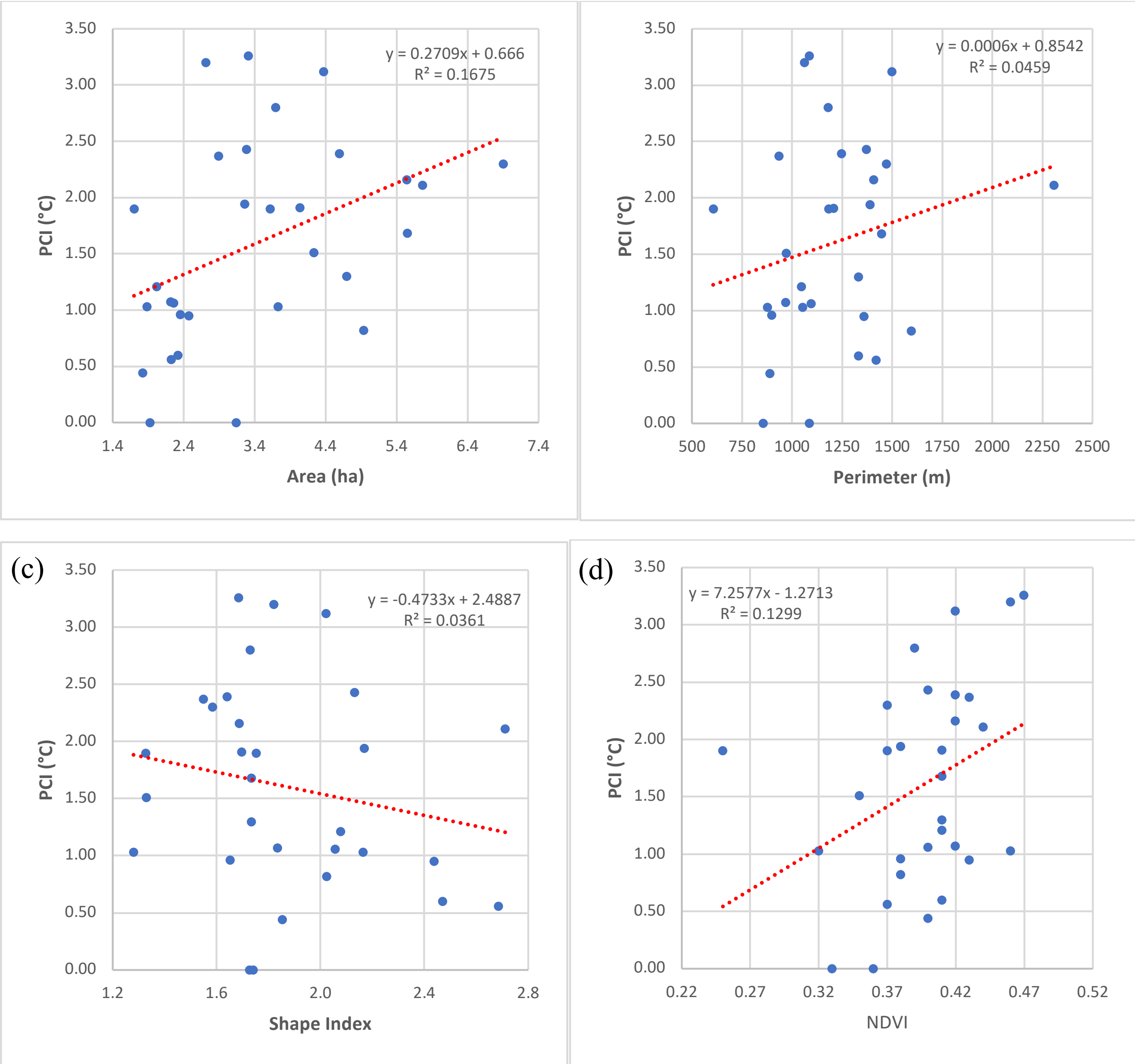

Figure 5.4 Regression analysis among PCI and park characteristics: (a) Area; (b) Perimeter; (c) Shape Index; (d) NDVI

According to the results obtained, it can be understood that the correlation between the park characteristics (area, perimeter, shape index and NDVI) and PCE can be complex and context dependent. The relationship may vary based on factors such as the park design, vegetation types in parks, surrounding urban environment and wind conditions. Although when each parameter is explored to its potential cooling effects, we can tell that with:

i. **Area:** Parks with larger area generally have more natural landscape with more green space and vegetation which can contribute to more significant cooling benefits. There may be more reduced heat absorption compared to smaller parks.

ii. **Perimeter:** The perimeter of a park could indirectly impact the cooling effects of an urban by

iii. **Shape Index**: The shape index of represents the shape complexity of park. Higher shape index values indicate more irregular shapes, while lower values more compact shapes such as the value of 1 indicates that the park is of a circular shape (Cao et al., 2010b). Therefore parks with the decrease in shape index values have a more concentrated green area optimizing the cooling benefits hence there can be an increase in PCE.

iv. **NDVI:** Higher NDVI values indicates greater abundance of green vegetation. As vegetation can provide shading and evapotranspiration, increase in NDVI therefore increases the parks cooling effect.

5.3. Impact of Urban Form on PCE

It is important to note that the PCE can be influence by external factors too. Specifically, the spatial characteristics in vertical direction surrounding urban parks. Obstructions, such as buildings may affect the dispersion of cool air. To quantify the influence of three-dimensional spatial characteristics and PCI around the urban parks, four urban form parameters (Building height (MBH), Floor Area Ratio (FAR), Aspect ratio (H/W) and Sky View Factor (SVF)) were examined in selected urban parks of various LCZ classes. Since calculating the urban morphology parameters like Canyon Aspect Ratio and SVF in all 30 parks requires a lot of computational process, manual work, and due to time constraint, the urban form of the 30 selected parks were evaluated using the LCZ classification with estimated values of AR and SVF values.

5.3.1. PCE on LCZ Classes

The LCZ classes varies in Glasgow City although most of the residential areas tend to have homogeneous urban fabric. Here, the LCZ classes surrounding the 30 urban parks were analysed and their relationship with PCI was examined. Majority of the urban parks fell into LCZ classes 8 and 9 which is ‘largely low-rise’ and ‘sparsely built’. Residential area is seen to be of low rise and sparsely built while commercial and industrial area are seen as largely low rise. The urban fabric of Glasgow tends to be homogeneous especially the residential area as you move away from the city centre where LCZ comprises of 2 and 3. According to relationship of PCI and surrounding LCZ of parks, it is noticed that PCI was higher in low rise areas.

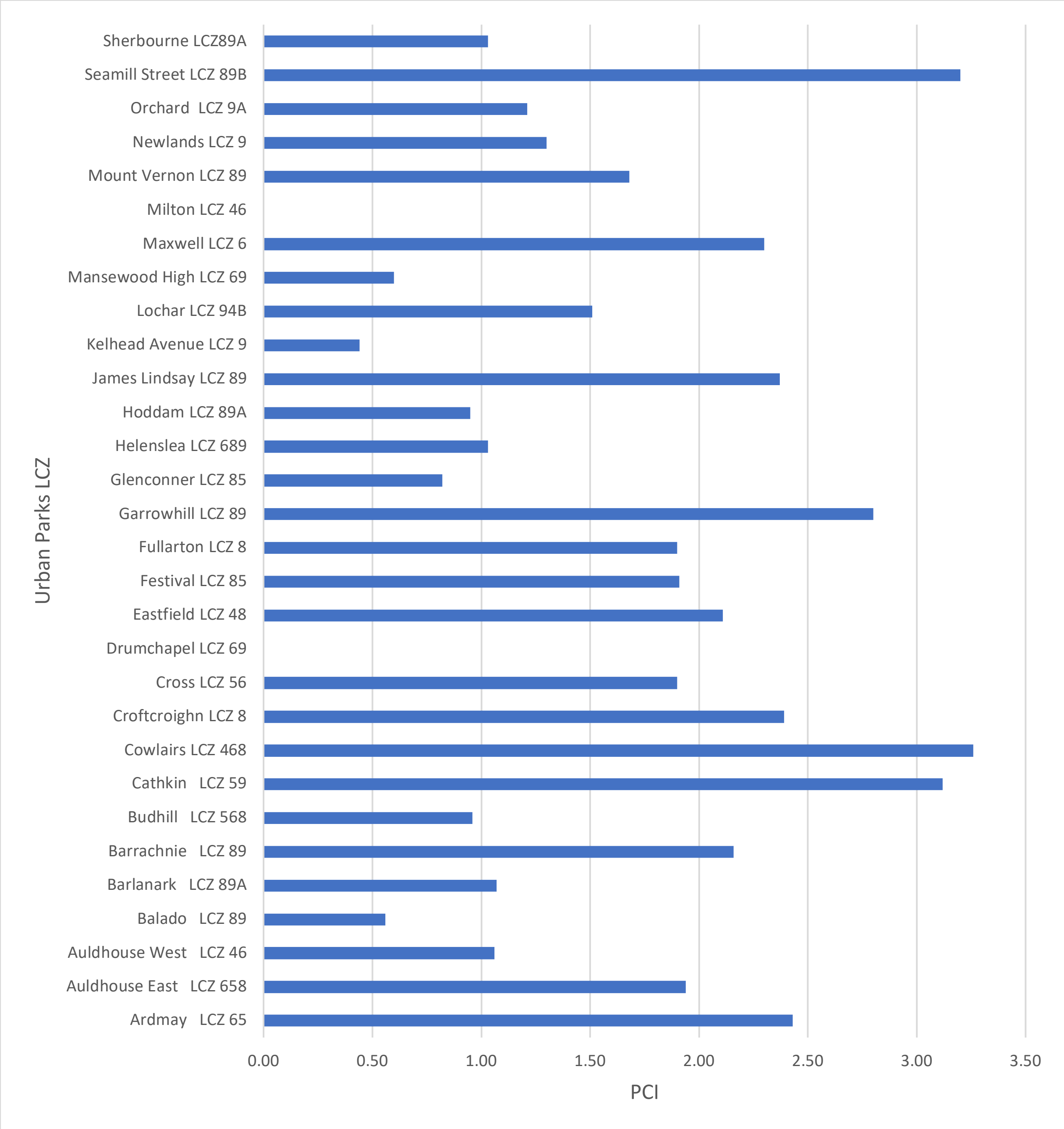

Figure 5.5 PCI between variation of LCZ classes

5.3.2. Influence of Urban Form around Urban Parks

Pearson's correlation analysis was used to assess the relationship between the urban parks PCI and urban morphology parameters while regression analysis was done between PCI and urban form parameters. Table 5.2 below shows the correlation analysis results obtained.

Table 5.2 The correlation between PCI and urban morphological parameters

	PCI	
	Pearson correlation	**Significance (2 tailed)**
MBH	-0.0232	0.5890
FAR	0.03584	0.6871
H/W	-0.0381	0.7882
SVF	-0.1870	0.2738

n = 30

As it was previously discussed, the surrounding urban form can significantly affect the cooling effects of parks in several ways. With correlation analysis between PCI, the quantitative impact was obtained. The results obtained highlighted the effects of urban form on PCE; Mean Building Height (MBH), Aspect Ratio (H/W) and SVF was negatively correlated with PCI as shown in Table 5.2 suggesting the PCI would decrease with the increase in building height, aspect ratio and SVF. If the parameters are examined individually, we are able to tell the following;

i. **MBH:** The increase in MBH can reduce the PCE since buildings with higher height may reduce the PCE of urban parks as they may block the spreading of cool air and ventilation. Adequate ventilation is crucial for dissipating heat and maintaining thermal comfort.
ii. **FAR**: FAR indicates the ratio of a buildings total floor area to the total area of the plot of land on which the building is constructed. FAR is generally used as a measure of urban density. The correlation of FAR to PCI showed a positive value indicating that the increase in FAR also increases the potential cooling effect of an urban park.
iii. **SVF**: High SVF values can indicate that more of the sky is visible from the ground and that there is less shading of buildings or trees. Therefore, the surrounding built environment of a park is likely to receive more direct sunlight leading to higher solar radiation and potential heat absorption which may affect the parks cooling potential.
iv. **H/W**: The canyon aspect ratio also known as the height to width ration of urban canyon may have both the effect of MBH and SVF parameters. High aspect ratio indicates that the buildings are tall and close to each other creating narrow streets. High values of H/W decrease the parks potential cooling effect as tall building together with heat-

absorbing surfaces tend to trap and retain heat, increasing the Urban Heat Island (UHI) effects.

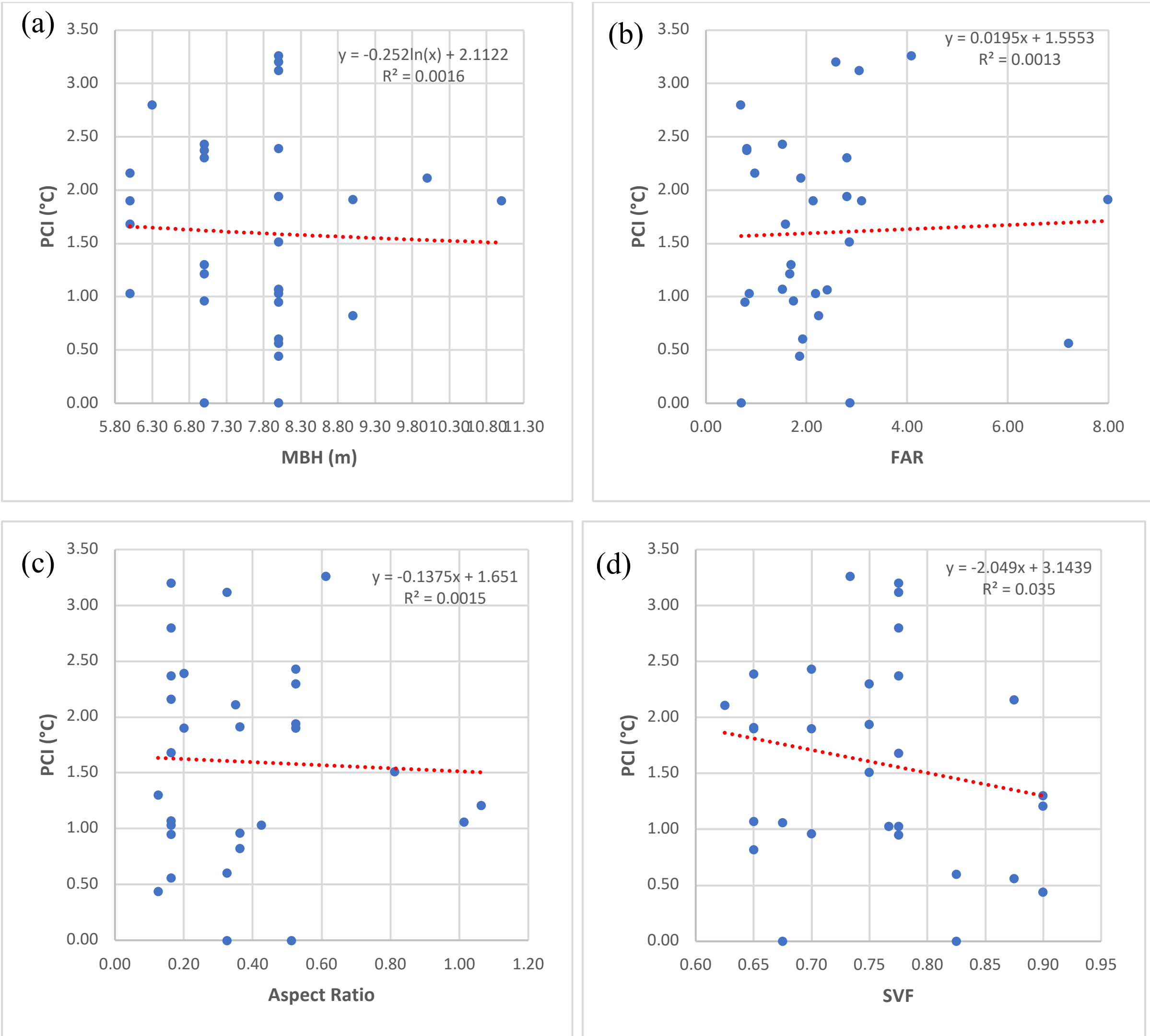

Figure 5.6 Regression analysis between PCI and urban form parameters

5.4. Implications

With the increasing impact of global warming, green spaces have become a crucial part of urban amenities affecting thermal comfort in urban areas. With this study, it is evident that urban parks reduce hot ambient temperatures in cities during summer. It is also noted that not only the park characteristics but also the surrounding built up around urban parks area can significantly affect the magnitude of Park Cooling Intensity (PCI). Although, it is also important to consider factors that contribute to strengthening the PCI of urban parks to achieve park cooling effects even with the smallest park area when designing urban parks. Therefore, measuring PCE of parks effectively can provide a scientific justification for better urban park planning to mitigate UHI effects.

The results achieved in this study can aid researchers, urban planners, and policy makers in understanding the Park Cooling Intensity (PCI) formation and Park Cooling Distance (PCD) threshold while acting as practical guideline to design urban parks with optimal cooling effect for mitigation of UHI in different urban forms. Understanding the impacts of urban form on the cooling potential of parks can help cities achieve a more sustainable and resilient urban environments. Additionally, promoting equitable access to cooling is crucial in areas of higher heat vulnerability especially to the socioeconomically disadvantaged communities (Tan and Samsudin, 2017b).

CHAPTER 6. CONCLUSIONS AND RECOMMENDATIONS

6.1. Conclusions

Cooling potential of urban parks in Glasgow city was assessed by two parameters in this study: (1) The Park Cooling Intensity (PCI), which is the maximum reduction in air temperature caused by the urban parks and (2) The Park Cooling Distance (PCD), which is the maximum cooling range of urban parks. Remote Sensing technique, GIS and Statistical analysis were used in this study to analyse the influence of park cooling effect with park characteristics and urban form during summer and evaluate its relationship. Additionally, LCZ scheme was used to support a methodology in analysing the influence of urban form on PCE of urban parks. Buffer analysis was used to measure the Park Cooling Intensity (PCI) and the Park Cooling Distance (PCD). Furthermore, urban form around the selected urban park samples were explored using three-dimensional urban morphology parameters derived from Ordnance Survey and LCZ framework.

It was found out that the average internal temperature of urban parks was lower than that of the surrounding built up area. At the same time, the correlation analysis revealed that the cooling effect of parks is considerably affected by its physical characteristics, such as the size and the shape of the park, canopy intensity, and the building density surrounding the park.

This study has confirmed that PCE is influenced by urban form as well as park characteristics. It also highlights the main results as follows:

- The average cooling intensity of 30 urban parks of an area between 1.3 ha to 6.9 ha was 1.6°C while the average cooling distance was 252.67m
- Urban parks area and perimeter had a positive relationship which indicates that it was an important factor in PCE. However, it does not necessarily mean that the increase in park maximizes the PCE. Although it can be confirmed that an increase in park size can be significant way to increase PCI while mitigating UHI effects.
- Similarly, NDVI showed a positive correlation with PCI indicating that with the increase of vegetation there is an increase in PCE.
- The shape Index had a negative correlation with PCI showing that the less complex the shape of a park is the more the greater the potential cooling effect.

- According to the relationship of LCZ and PCI, it was noticed that PCE was higher in LCZ 8 and 9 where the urban fabric is of low rise and sparsely built.
- Urban form parameters such as MBH, H/W, SVF had a negative correlation with PCI suggesting that the increase in building height, aspect ratio and SVF can decrease the potential cooling effect of urban parks.

6.2. Limitations

Although this study presented measurement methods and assessed the relationship between PCE and urban form, there are several limitations that should be discussed. As this research was carried using remote sensing technique only, it is by itself limiting. Other limitations are highlighted as follows:

- This study focused only on one summer season in daytime, which can be restricting, whereas there are seasonal variations in UHI and urban cooling effects.
- The of LST without correlating with air temperature may yield different results.
- The number and size of parks taken for this study is limited. Urban dynamics are complex; therefore, it is required to analyse large samples of data to accurately understand the scale of PCE as the small number of sample results in a limited spatial and temporal scale.
- The data used in this study is focused on a mixed urban form during summer, although this does not give the assumptions that all urban areas of this type will experience the same effect on the PCE as illustrated.
- The material composition of urban envelopes can have a significant effect on urban microclimates however, this study only compared three dimensional characteristics of urban form as variables.
- The urban fabric in Glasgow city, especially the residential areas tend to be quite homogeneous, therefore the impact of the findings does not show a wide variation.
- Fieldwork measurements was not done in this study therefore relying only on remote sensing can be limiting.
- The use of different data sources obtained to calculate the urban form parameters such as the Aspect Ratio and SVF could lead to different results.
- Correlation analysis method is limited as the relationship of PCE is not a linear relationship.

6.3. Recommendations for Further Studies

The cooling effect of urban parks is an evolving topic hance further studies need to be conducted across different spatial forms to further refine the research findings. Additionally, the following recommendations are proposed:

- The research needs to be done across seasonal and latitude variations to be considered for development of planning recommendations.
- By analysing the existing urban form, the neighbourhood surrounding the urban parks can be taken to perform scenario-based simulations to explore the interaction between urban form, wind and PCE
- With scenario-based simulations, further study can be taken to explore different threshold values of PCE
- The relationship of PCI and park characteristics, especially the size is seen to be non-linear which suggests that when the PCI reaches a certain threshold the values may remain constant. Due to this, further research needs to be taken to explore the threshold of the cooling range in various park sizes.
- Further research needs to be conducted in a more heterogeneous urban environment and climate zones.

REFERENCES

1) 68% of the world population projected to live in urban areas by 2050, says UN | UN DESA | United Nations Department of Economic and Social Affairs (no date). Available at: https://www.un.org/development/desa/en/news/population/2018-revision-of-world-urbanization-prospects.html (Accessed: 1 July 2023).
2) Adaptation Scotland :: Climate trends and projections (no date). Available at: https://www.adaptationscotland.org.uk/why-adapt/climate-trends-and-projections%20 (Accessed: 27 March 2023).
3) Akbari, H. and Kolokotsa, D. (2016) 'Three decades of urban heat islands and mitigation technologies research', Energy and Buildings, 133, pp. 834–842. Available at: https://doi.org/10.1016/J.ENBUILD.2016.09.067.
4) Aslam, A., Rana, I.A. and Bhatti, S.S. (2021) 'The spatiotemporal dynamics of urbanisation and local climate: A case study of Islamabad, Pakistan', Environmental Impact Assessment Review, 91, p. 106666. Available at: https://doi.org/10.1016/J.EIAR.2021.106666.
5) Cao, X. et al. (2010a) 'Quantifying the cool island intensity of urban parks using ASTER and IKONOS data', Landscape and Urban Planning, 96(4), pp. 224–231. Available at: https://doi.org/10.1016/J.LANDURBPLAN.2010.03.008.
6) Cao, X. et al. (2010b) 'Quantifying the cool island intensity of urban parks using ASTER and IKONOS data', Landscape and Urban Planning, 96(4), pp. 224–231. Available at: https://doi.org/10.1016/J.LANDURBPLAN.2010.03.008.
7) Chen, M. et al. (2022) 'Quantification and mapping cooling effect and its accessibility of urban parks in an extreme heat event in a megacity', Journal of Cleaner Production, 334, p. 130252. Available at: https://doi.org/10.1016/j.jclepro.2021.130252.
8) Chen, Y.C. et al. (2019) 'Interpreting air temperature generated from urban climatic map by urban morphology in Taipei', Theoretical and Applied Climatology, 137(3–4), pp. 2657–2662. Available at: https://doi.org/10.1007/S00704-018-02764-X/METRICS.
9) CLIMATE PROOFING GLASGOW Adaptation Strategies for Urban Overheating (no date).
10) Degirmenci, K. et al. (2021) 'Understanding policy and technology responses in mitigating urban heat islands: A literature review and directions for future research', Sustainable Cities and Society, 70, p. 102873. Available at: https://doi.org/10.1016/J.SCS.2021.102873.

11) Deilami, K., Kamruzzaman, M. and Liu, Y. (2017) 'Urban heat island effect: A systematic review of spatio-temporal factors, data, methods, and mitigation measures'. Available at: https://doi.org/10.1016/j.jag.2017.12.009.
12) Dousset, B. and Gourmelon, F. (2003) 'Satellite multi-sensor data analysis of urban surface temperatures and landcover', ISPRS Journal of Photogrammetry and Remote Sensing, 58(1–2), pp. 43–54. Available at: https://doi.org/10.1016/S0924-2716(03)00016-9.
13) Emmanuel, R. et al. (2023a) 'Urban Heat Risk: Protocols for Mapping and Implications for Colombo, Sri Lanka', Atmosphere 2023, Vol. 14, Page 343, 14(2), p. 343. Available at: https://doi.org/10.3390/ATMOS14020343.
14) Emmanuel, R. et al. (2023b) 'Urban Heat Risk: Protocols for Mapping and Implications for Colombo, Sri Lanka', Atmosphere 2023, Vol. 14, Page 343, 14(2), p. 343. Available at: https://doi.org/10.3390/ATMOS14020343.
15) Emmanuel, R.; and Loconsole, A. (no date) 'Green infrastructure as an adaptation approach to tackling urban overheating in the Glasgow Clyde Valley Region, UK'. Available at: https://doi.org/10.1016/j.landurbplan.2015.02.012.
16) Ewers, R.M. and Didham, R.K. (2007) 'The effect of fragment shape and species' sensitivity to habitat edges on animal population size: Contributed papers', Conservation Biology, 21(4), pp. 926–936. Available at: https://doi.org/10.1111/J.1523-1739.2007.00720.X.
17) Excess mortality during heat-periods - Office for National Statistics (no date). Available at: https://www.ons.gov.uk/peoplepopulationandcommunity/birthsdeathsandmarriages/deaths/articles/excessmortalityduringheatperiods/englandandwales1juneto31august2022 (Accessed: 26 May 2023).
18) Geng, X. et al. (2022) 'The influence of local background climate on the dominant factors and threshold-size of the cooling effect of urban parks'. Available at: https://doi.org/10.1016/j.scitotenv.2022.153806.
19) Gunawardena, K.R., Wells, M.J. and Kershaw, T. (2017) 'Utilising green and bluespace to mitigate urban heat island intensity'. Available at: https://doi.org/10.1016/j.scitotenv.2017.01.158.
20) Hämmerle, M. et al. (no date) INTRODUCING A SCRIPT FOR CALCULATING THE SKY VIEW FACTOR USED FOR URBAN CLIMATE INVESTIGATIONS.

21) Homewood, P. (2023) 'T H E U K ' S W E AT H E R I N 2 0 2 2 Paul Homewood The UK's Weather in 2022'.
22) Id, H.T., Zinzi, M. and Santamouris, M. (2017) 'Influence of Urban Green Area on Air Temperature of Surrounding Built-Up Area', Climate 2017, Vol. 5, Page 60, 5(3), p. 60. Available at: https://doi.org/10.3390/CLI5030060.
23) Kamboj, S. and Ali, S. (2021) 'Urban sprawl of Kota city: A case study of urban heat island linked with electric consumption Selection and peer-review under responsibility of the scientific committee of the International Confer-ence on Innovations in Clean Energy Technologies'. Available at: https://doi.org/10.1016/j.matpr.2020.08.783.
24) Konijnendijk, C.C. et al. (2013) 'Benefits of Urban Parks - A systematic review', International Federation of Parks and Recreation Administration, (January), pp. 1–68.
25) Lee, H., Mayer, H. and Chen, L. (2016) 'Contribution of trees and grasslands to the mitigation of human heat stress in a residential district of Freiburg, Southwest Germany', Landscape and Urban Planning, 148, pp. 37–50. Available at: https://doi.org/10.1016/j.landurbplan.2015.12.004.
26) Li, X. et al. (2012) 'Spatial pattern of greenspace affects land surface temperature: Evidence from the heavily urbanized Beijing metropolitan area, China', Landscape Ecology, 27(6), pp. 887–898. Available at: https://doi.org/10.1007/s10980-012-9731-6.
27) Lin, W. et al. (2015a) 'Calculating cooling extents of green parks using remote sensing: Method and test', Landscape and Urban Planning, 134, pp. 66–75. Available at: https://doi.org/10.1016/j.landurbplan.2014.10.012.
28) Lin, W. et al. (2015b) 'Calculating cooling extents of green parks using remote sensing: Method and test', Landscape and Urban Planning, 134, pp. 66–75. Available at: https://doi.org/10.1016/J.LANDURBPLAN.2014.10.012.
29) Lin, W. et al. (2015c) 'Calculating cooling extents of green parks using remote sensing: Method and test', Landscape and Urban Planning, 134, pp. 66–75. Available at: https://doi.org/10.1016/J.LANDURBPLAN.2014.10.012.
30) Liu, X. et al. (2022) 'Influences of landform and urban form factors on urban heat island: Comparative case study between Chengdu and Chongqing'. Available at: https://doi.org/10.1016/j.scitotenv.2022.153395.
31) Park, J. et al. (2017) 'The influence of small green space type and structure at the street level on urban heat island mitigation', Urban Forestry & Urban Greening, 21, pp. 203–212. Available at: https://doi.org/10.1016/j.ufug.2016.12.005.

32) Peel, M.C., Finlayson, B.L. and Mcmahon, T.A. (2007) Hydrology and Earth System Sciences Updated world map of the Köppen-Geiger climate classification, Hydrol. Earth Syst. Sci.
33) Power, S.B. and D Delage, F.P. (no date) 'Setting and smashing extreme temperature records over the coming century', Nature Climate Change [Preprint]. Available at: https://doi.org/10.1038/s41558-019-0498-5.
34) Ren, Z. et al. (2013) 'Estimation of the Relationship between Urban Park Characteristics and Park Cool Island Intensity by Remote Sensing Data and Field Measurement', 4, pp. 868–886. Available at: https://doi.org/10.3390/f4040868.
35) Saunders, M.N.K., Lewis, P. and Thornhill, A. (2019) Chapter 4: Understanding research philosophy and approaches to theory development, Research Methods for Business Studies.
36) Shashua-Bar, L., Pearlmutter, D. and Erell, E. (2011) 'The influence of trees and grass on outdoor thermal comfort in a hot-arid environment', International Journal of Climatology, 31(10), pp. 1498–1506. Available at: https://doi.org/10.1002/JOC.2177.
37) statistics.gov.scot | Glasgow City (no date). Available at: https://statistics.gov.scot/atlas/resource?uri=http%3A%2F%2Fstatistics.gov.scot%2Fid%2Fstatistical-geography%2FS12000049 (Accessed: 19 April 2023).
38) Stewart, I.D. and Oke, T.R. (2012) 'Local Climate Zones for Urban Temperature Studies', Bulletin of the American Meteorological Society, 93(12), pp. 1879–1900. Available at: https://doi.org/10.1175/BAMS-D-11-00019.1.
39) Sugawara, H. et al. (2016) 'Thermal Influence of a Large Green Space on a Hot Urban Environment', Journal of environmental quality, 45(1), pp. 125–133. Available at: https://doi.org/10.2134/JEQ2015.01.0049.
40) Tan, P.Y. and Samsudin, R. (2017a) 'Effects of spatial scale on assessment of spatial equity of urban park provision', Landscape and Urban Planning, 158, pp. 139–154. Available at: https://doi.org/10.1016/J.LANDURBPLAN.2016.11.001.
41) Tan, P.Y. and Samsudin, R. (2017b) 'Effects of spatial scale on assessment of spatial equity of urban park provision', Landscape and Urban Planning, 158, pp. 139–154. Available at: https://doi.org/10.1016/J.LANDURBPLAN.2016.11.001.
42) Toparlar, Y. et al. (2018) 'The effect of an urban park on the microclimate in its vicinity: a case study for Antwerp, Belgium', International Journal of Climatology, 38, pp. e303–e322. Available at: https://doi.org/10.1002/JOC.5371.

43) Undorf, S. et al. (2020) ‘Learning from the 2018 heatwave in the context of climate change: Are high-temperature extremes important for adaptation in Scotland?’, Environmental Research Letters, 15. Available at: https://doi.org/10.1088/1748-9326/ab6999.
44) Wang, X. et al. (2021) ‘Tree species richness and diversity predicts the magnitude of urban heat island mitigation effects of greenspaces’, Science of the Total Environment, 770. Available at: https://doi.org/10.1016/J.SCITOTENV.2021.145211.
45) Wang, Y. and Akbari, H. (2016) ‘The effects of street tree planting on Urban Heat Island mitigation in Montreal’, Sustainable Cities and Society, 27, pp. 122–128. Available at: https://doi.org/10.1016/J.SCS.2016.04.013.
46) Yu, Z. et al. (2017a) ‘How can urban green spaces be planned for climate adaptation in subtropical cities?’ Available at: https://doi.org/10.1016/j.ecolind.2017.07.002.
47) Yu, Z. et al. (2017b) ‘How can urban green spaces be planned for climate adaptation in subtropical cities?’, Ecological Indicators, 82, pp. 152–162. Available at: https://doi.org/10.1016/J.ECOLIND.2017.07.002.
48) Zhang, J., Gou, Z. and Lu, Y. (2021) ‘Outdoor thermal environments and related planning factors for subtropical urban parks’, Indoor and Built Environment, 30(3), pp. 363–374. Available at: https://doi.org/10.1177/1420326X19891462/ASSET/IMAGES/LARGE/10.1177_1420326X19891462-FIG2.JPEG.
49) Zhao, C. et al. (2011) ‘Urban planning indicators, morphology and climate indicators: A case study for a north-south transect of Beijing, China’, Building and Environment, 46(5), pp. 1174–1183. Available at: https://doi.org/10.1016/J.BUILDENV.2010.12.009.

APPENDICES

APPENDIX A: Fitted curves results of 30 urban parks between Tmax and Lmax

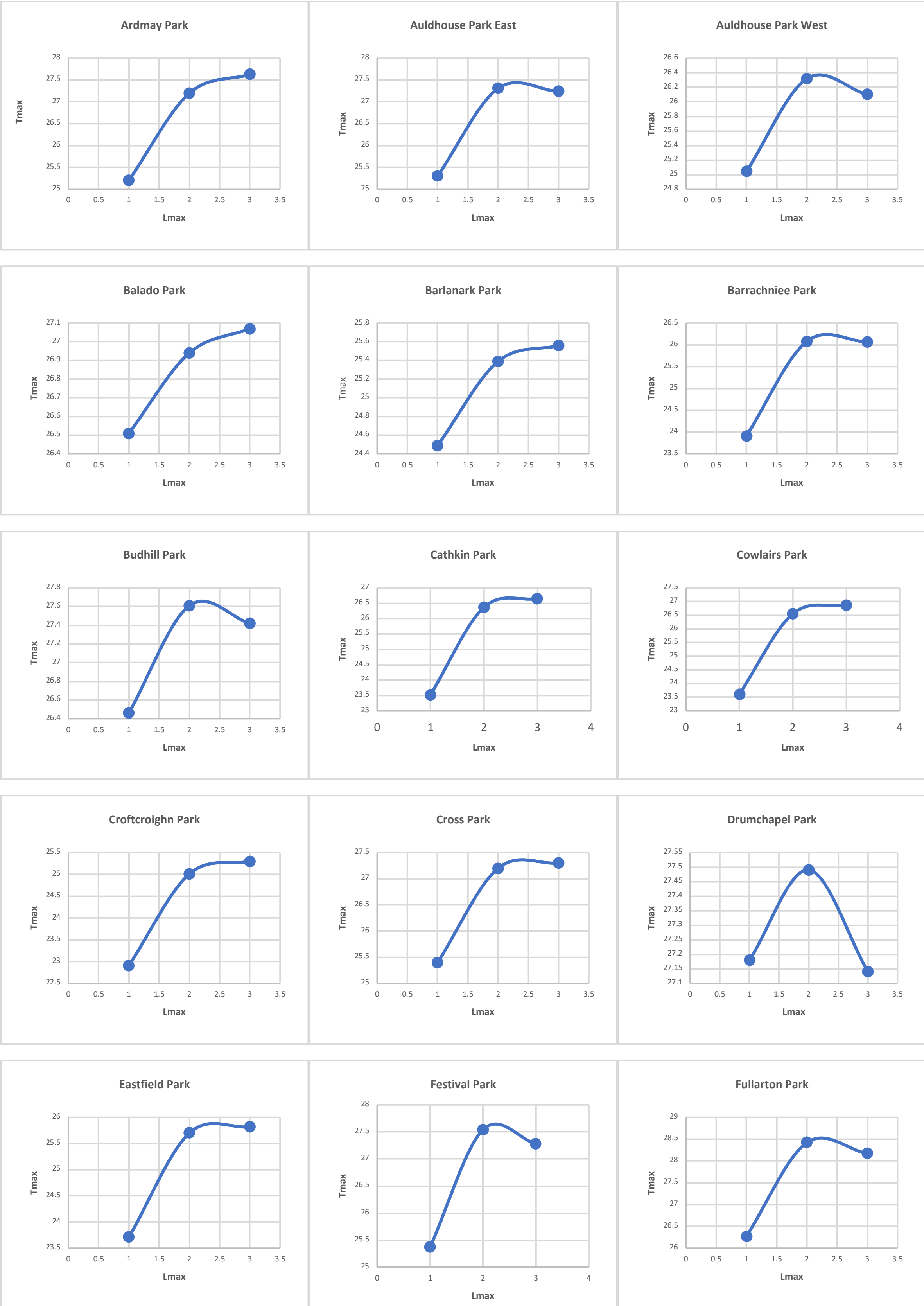


Garrowhill Park
28
27.5
27
26.5
26
25.5
25
24.5
Tmax
0 0.5 1 1.5 2 2.5 3 3.5
Lmax

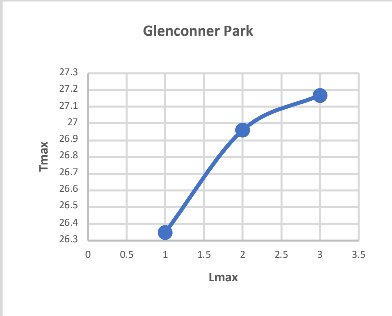
Glenconner Park
27.3
27.2
27.1
27
26.9
26.8
26.7
26.6
26.5
26.4
26.3
Tmax
0 0.5 1 1.5 2 2.5 3 3.5
Lmax

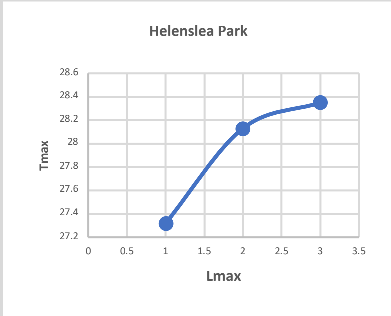
Helenslea Park
28.6
28.4
28.2
28
27.8
27.6
27.4
27.2
Tmax
0 0.5 1 1.5 2 2.5 3 3.5
Lmax

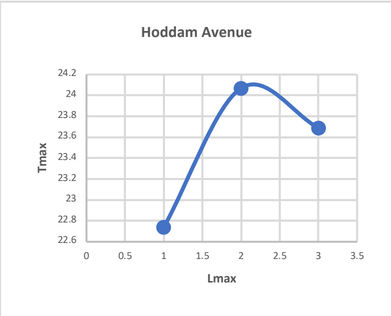
Hoddam Avenue
24.2
24
23.8
23.6
23.4
23.2
23
22.8
22.6
Tmax
0 0.5 1 1.5 2 2.5 3 3.5
Lmax

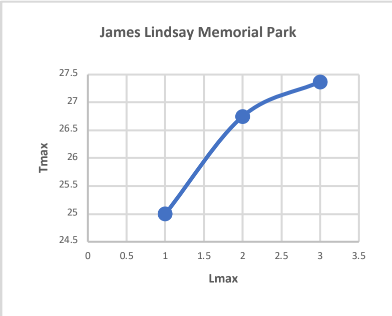
James Lindsay Memorial Park
27.5
27
26.5
26
25.5
25
24.5
Tmax
0 0.5 1 1.5 2 2.5 3 3.5
Lmax

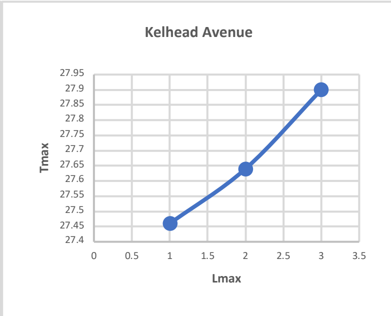
Kelhead Avenue
27.95
27.9
27.85
27.8
27.75
27.7
27.65
27.6
27.55
27.5
27.45
27.4
Tmax
0 0.5 1 1.5 2 2.5 3 3.5
Lmax

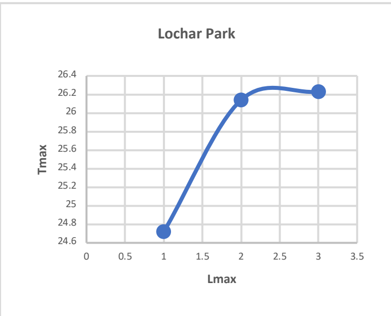
Lochar Park
26.4
26.2
26
25.8
25.6
25.4
25.2
25
24.8
24.6
Tmax
0 0.5 1 1.5 2 2.5 3 3.5
Lmax

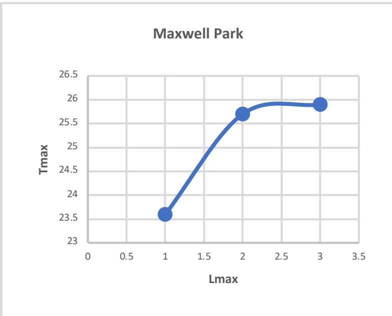
Maxwell Park
26.5
26
25.5
25
24.5
24
23.5
23
Tmax
0 0.5 1 1.5 2 2.5 3 3.5
Lmax

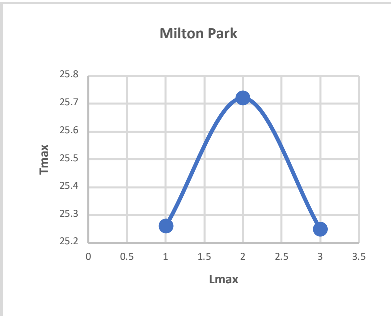
Milton Park
25.8
25.7
25.6
25.5
25.4
25.3
25.2
Tmax
0 0.5 1 1.5 2 2.5 3 3.5
Lmax

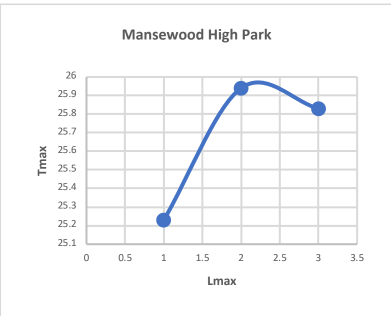
Mansewood High Park
26
25.9
25.8
25.7
25.6
25.5
25.4
25.3
25.2
25.1
Tmax
0 0.5 1 1.5 2 2.5 3 3.5
Lmax

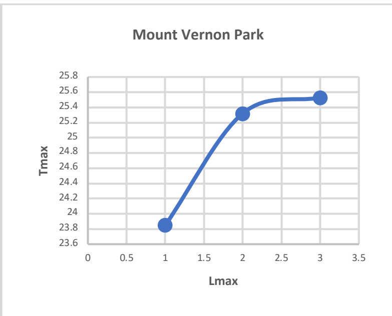
Mount Vernon Park
25.8
25.6
25.4
25.2
25
24.8
24.6
24.4
24.2
24
23.8
23.6
Tmax
0 0.5 1 1.5 2 2.5 3 3.5
Lmax

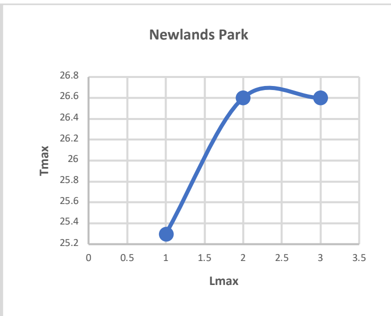
Newlands Park
26.8
26.6
26.4
26.2
26
25.8
25.6
25.4
25.2
Tmax
0 0.5 1 1.5 2 2.5 3 3.5
Lmax

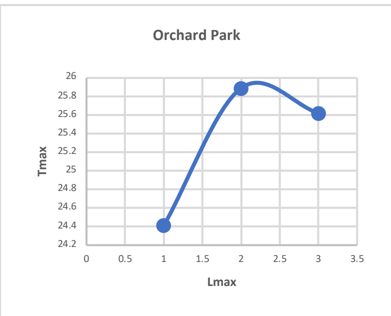
Orchard Park
26
25.8
25.6
25.4
25.2
25
24.8
24.6
24.4
24.2
Tmax
0 0.5 1 1.5 2 2.5 3 3.5
Lmax

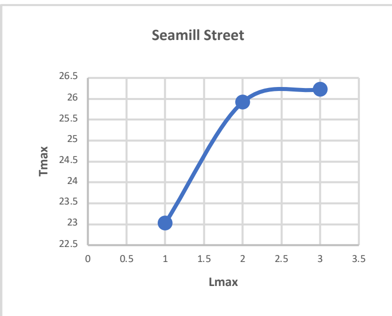
Seamill Street
26.5
26
25.5
25
24.5
24
23.5
23
22.5
Tmax
0 0.5 1 1.5 2 2.5 3 3.5
Lmax

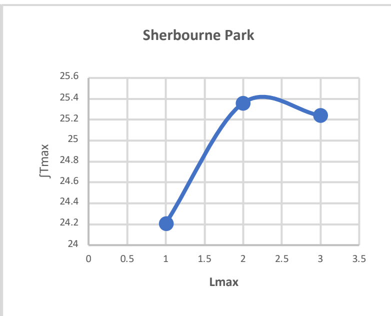
Sherbourne Park
25.6
25.4
25.2
25
24.8
24.6
24.4
24.2
24
Tmax
0 0.5 1 1.5 2 2.5 3 3.5
Lmax

APPENDIX B: Spatial Building Distribution around urban parks

Ardmay Park

Auldhouse Park East

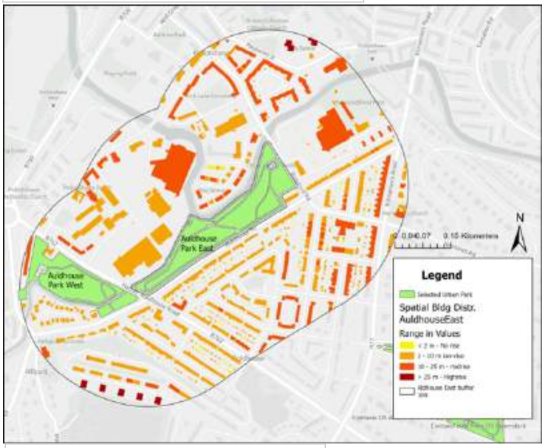

Auldhouse Park West

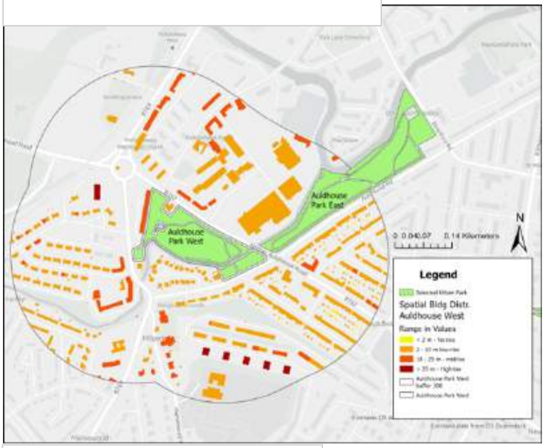

Balado Park

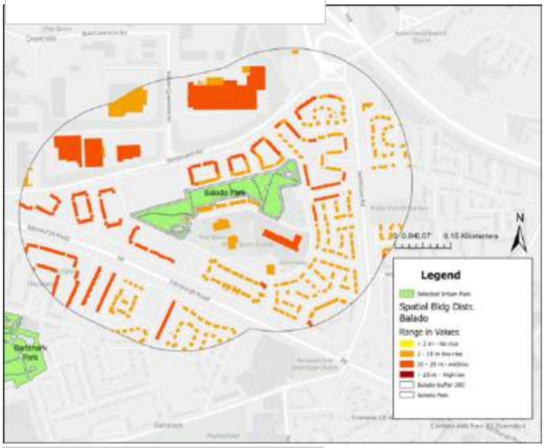

Barlanark Park

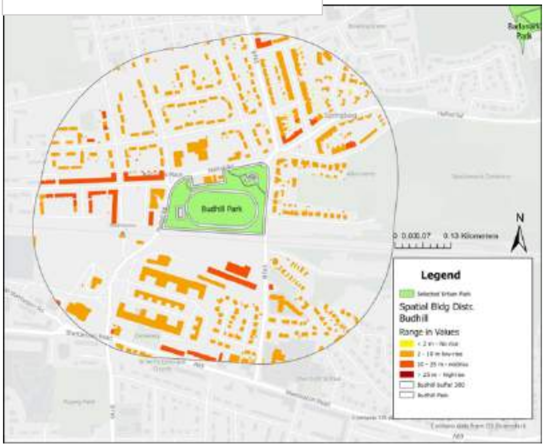

Barrachnie Park

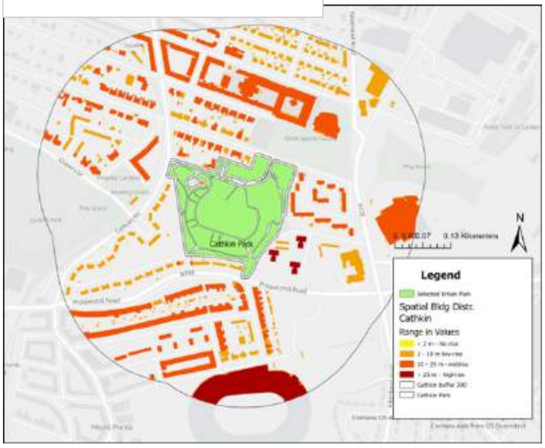

Budhill Park

Cathkin Park

Cowlairs Park

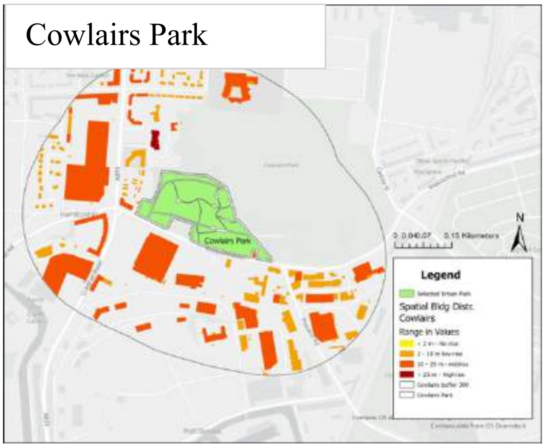

Croftcroighn Park

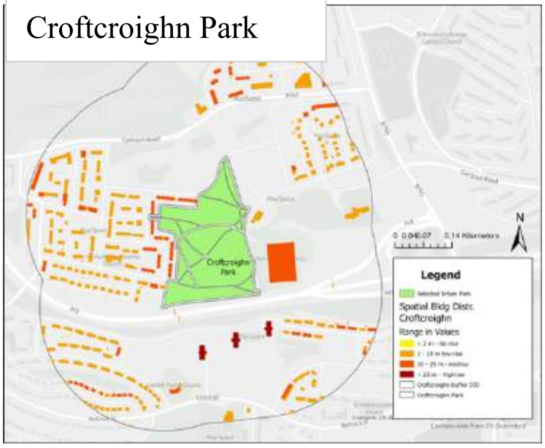

Cross Park

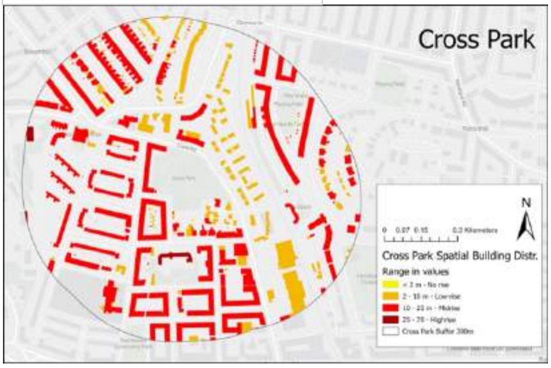

Drumchapel Park

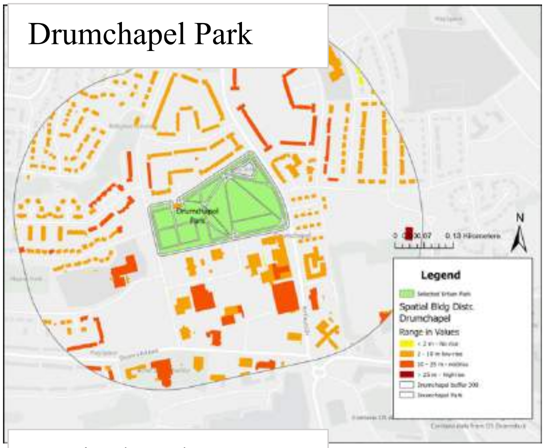

Eastfield Park

Festival Park

Fullarton Park

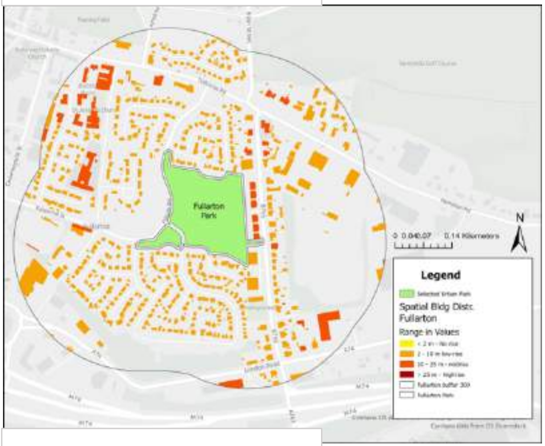

Garrowhill Park

Glenconner Park

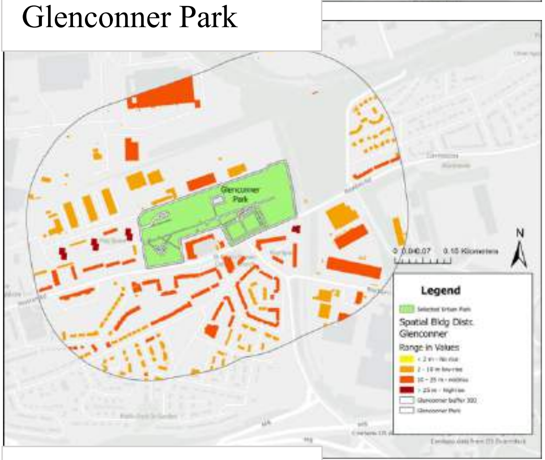

Helenslea Park

Hoddam Avenue

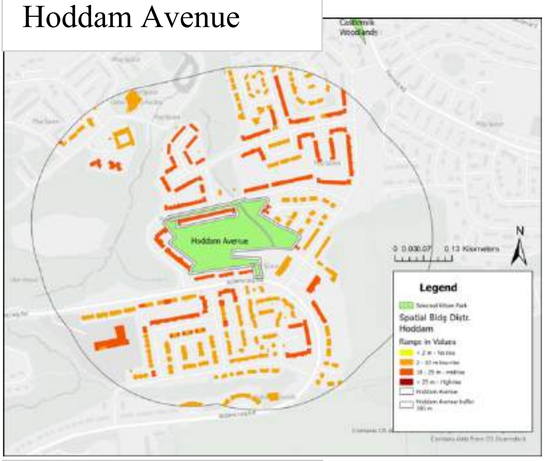

James Lindsay Memorial Park

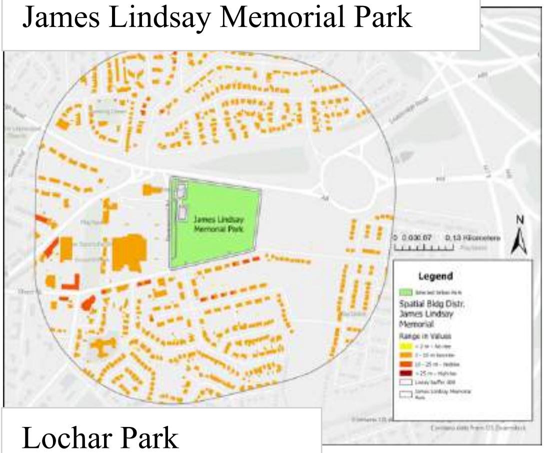

Kelhead Avenue

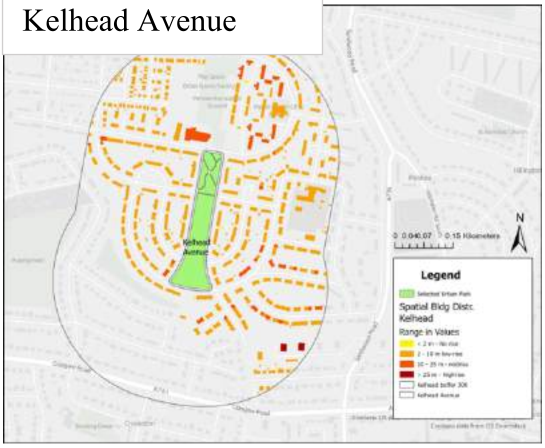

Lochar Park

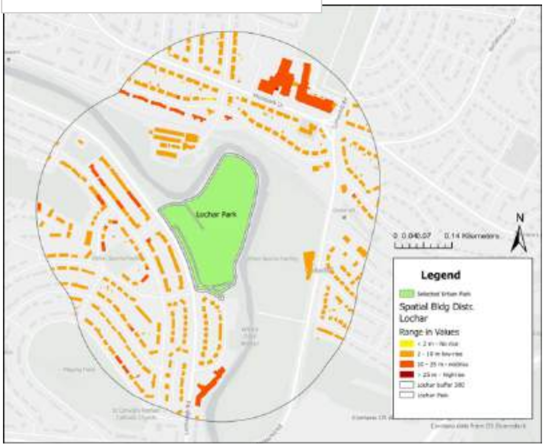

Mansewood High Park

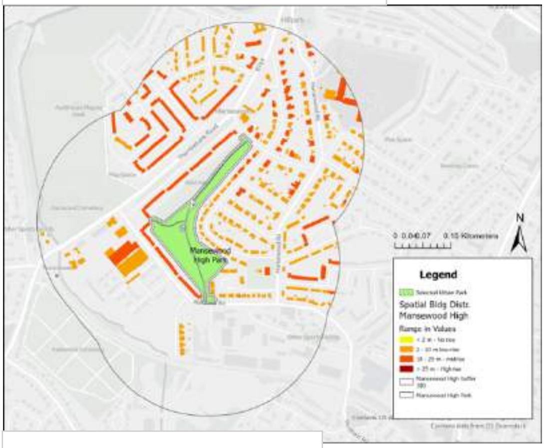

Maxwell Park

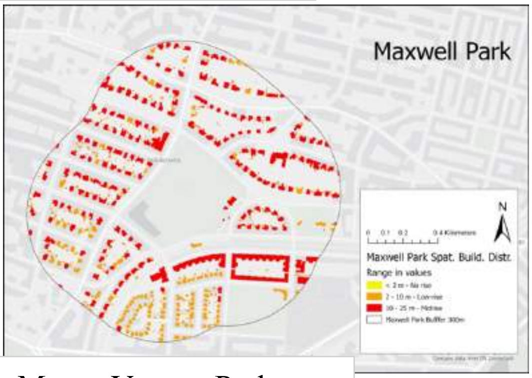

Milton Park

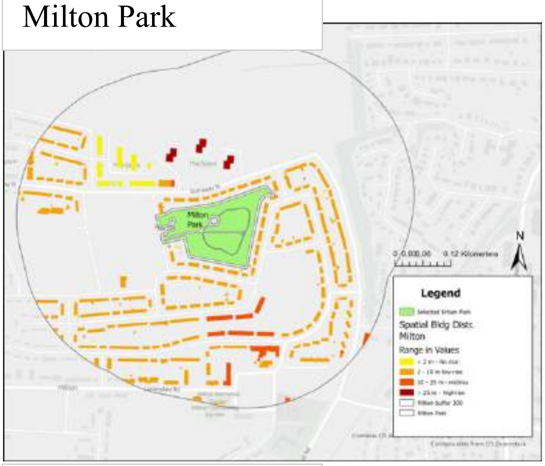

Mount Vernon Park

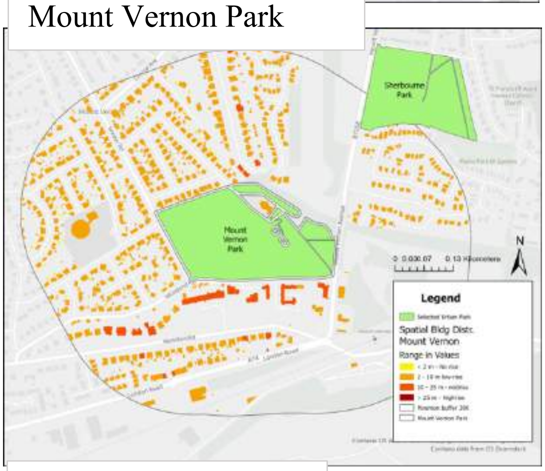

Newlands Park

Orchard Park

Seamill Street Park

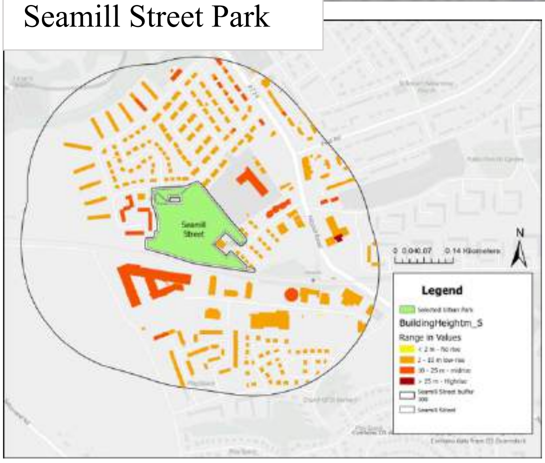

Sherbourne Park

APPENDIX C: Aerial images of selected urban parks surrounding urban form


(9) Hoddam Avenue


(10) Festival Park


(11) Mansewood High Park


(12) Drumchapel Park


(13) Kelhead Avenue


(14) Glenconner Park


(15) Cowlairs Park


(16) Milton Park


(17) Eastfield Park


(18) Lochar Park


(19) Barrachnie Park


(20) Sherbourne Park


(21) Mount Vernon Park


(22) Fullarton Park


(23) Helenslea Park


(24) Croftcroighn Park


(25) Auldhouse Park East


(26) Auldhouse Park West


(27) Seamill Street

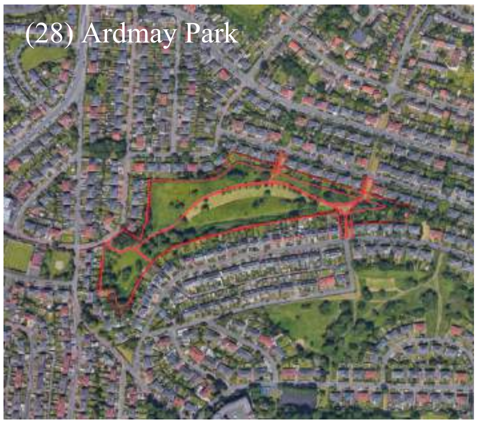
(28) Ardmay Park


(29) Cathkin Park


(30) Orchard Park